

Accretion Disks

H.C. Spruit

Max Planck Institute for Astrophysics,
Box 1317, 85741 Garching, Germany,
henk@mpa-garching.mpg.de

Abstract In this lecture the basic theory of accretion disks is reviewed, with emphasis on aspects relevant for X-ray binaries and Cataclysmic Variables. The text gives a general introduction as well as a selective discussion of a number of more recent topics.

1 Introduction

Accretion disks are inferred to exist as objects of very different scales: millions of km in low Mass X-ray Binaries (LMXB) and Cataclysmic Variables (CV), solar radius-to-AU scale disks in protostellar objects, and AU-to-parsec scale disks in Active Galactic Nuclei (AGN).

An interesting observational connection exists between accretion disks and jets (such as the spectacular jets from AGN and protostars), and outflows (the ‘CO-outflows’ from protostars and the ‘broad-line-regions’ in AGN). Lacking direct (i.e. spatially resolved) observations of disks, theory has tried to provide models, with varying degrees of success. Uncertainty still exists with respect to some basic questions. In this situation, progress made by observations or modeling of a particular class of objects has direct impact for the understanding of other objects, including the enigmatic connection with jets.

In this lecture I concentrate on the more basic aspects of accretion disks, but an attempt is made to mention topics of current interest as well. Some emphasis is on those aspects of accretion disk theory that connect to the observations of LMXB and CV’s. For other reviews on the basics of accretion disks, see Pringle (1981), Papaloizou and Lin (1995). For a more extensive introduction, the textbook by Frank et al. (2002). For a comprehensive text on CVs, Warner 1995.

2 Accretion: general

Gas falling into a point mass potential

$$\Phi = -\frac{GM}{r}$$

from a distance r_0 to a distance r converts gravitational into kinetic energy, by an amount $\Delta\Phi = GM(1/r - 1/r_0)$. For simplicity, assuming that the starting distance is large, $\Delta\Phi = GM/r$. The speed of arrival, the *free-fall speed* v_{ff} is given by

$$\frac{1}{2}v_{\text{ff}}^2 = GM/r. \quad (1)$$

If the gas is then brought to rest, for example at the surface of a star, the amount of energy e dissipated per unit mass is

$$e = \frac{1}{2}v_{\text{ff}}^2 = \frac{GM}{r} \quad (\text{rest}).$$

If, instead, it goes into a circular Kepler orbit at distance r :

$$e = \frac{1}{2} \frac{GM}{r} \quad (\text{orbit}).$$

The dissipated energy may go into internal energy of the gas, and into radiation which escapes to infinity (usually in the form of photons, but neutrino losses can also play a role in some cases).

2.1 Adiabatic accretion

Consider first the case when radiation losses are neglected. Any mechanical energy dissipated stays locally in the flow. This is called an *adiabatic* flow (not to be confused with *isentropic* flow). For an ideal gas with constant ratio of specific heats γ , the internal energy per unit mass is

$$e = \frac{P}{(\gamma-1)\rho}.$$

With the equation of state

$$P = \mathcal{R}\rho T/\mu \quad (2)$$

where \mathcal{R} is the gas constant and μ the mean atomic weight per particle, we find the temperature of the gas after the dissipation has taken place (assuming that the gas goes into a circular orbit):

$$T = \frac{1}{2}(\gamma-1)T_{\text{vir}}, \quad (3)$$

where T_{vir} , the *virial temperature* is defined as

$$T_{\text{vir}} = \frac{GM\mu}{\mathcal{R}r} = gr\mu/\mathcal{R},$$

where g is the acceleration of gravity at distance r . In an atmosphere with temperature near T_{vir} , the sound speed $c_s = (\gamma\mathcal{R}T/\mu)^{1/2}$ is close to the escape speed from the system, and the hydrostatic pressure scale height, $H \equiv \mathcal{R}T/(\mu g)$ is of the order of r . Such an atmosphere may evaporate on a relatively short time scale in the form of a stellar wind. This is as expected

from energy conservation: if no energy is lost through radiation, the energy gained by the fluid while falling into a gravitational potential is also sufficient to move it back out again.

A simple example is spherically symmetric adiabatic accretion (Bondi, 1952). An important result is that such accretion is possible only if $\gamma \leq 5/3$. The lower γ , the lower the temperature in the accreted gas (eq. 3), and the easier it is for the gas to stay bound in the potential. A classical situation where adiabatic and roughly spherical accretion takes place is a supernova implosion: when the central temperature becomes high enough for the radiation field to start disintegrating nuclei, γ drops and the envelope collapses onto the forming neutron star via an accretion shock. Another case are Thorne-Zytkow objects (e.g. Cannon et al. 1992), where γ can drop to low values due to pair creation, initiating an adiabatic accretion onto the black hole.

Adiabatic spherical accretion is fast, taking place on the dynamical time scale: something on the order of the free fall time scale, or Kepler orbital time scale,

$$\tau_d = r/v_K = \Omega_K^{-1} = (r^3/GM)^{1/2}, \quad (4)$$

where v_K , Ω_K are the Kepler orbital velocity and angular frequency.

When radiative loss becomes important, the accreting gas can stay cool irrespective of the value of γ , and Bondi's critical value $\gamma = 5/3$ plays no role. With such losses, the temperatures of accretion disks are usually much lower than the virial temperature.

2.2 Temperature near compact objects

For accretion onto a neutron star surface, $R = 10$ km, $M = 1.4M_\odot$, we have a free fall speed $v_{ff}/c \approx 0.4c$ (this in Newtonian approximation, the correct value in General Relativity is quantitatively somewhat different). The corresponding virial temperature would be $T_v \sim 2 \cdot 10^{12}$ K, equivalent to an average energy of 150 MeV per particle.

This is not the actual temperature we should expect, since other things happen before such temperatures are reached. If the accretion is adiabatic, one of these is the creation of a very dense radiation field. The energy liberated per infalling particle is still the same, but it gets shared with a large number of photons. At temperatures above the electron rest mass ($\approx 0.5MeV$), electron-positron pairs e^\pm are produced in addition to photons. These can take up most of the accretion energy, limiting the temperature typically to a few MeV.

In most observed disks temperatures do not get even close to an MeV, however, because accretion is rarely adiabatic. Energy loss takes place by escaping photons (or under more extreme conditions: neutrinos). Exceptions are the radiatively inefficient accretion flows discussed in section 13.

2.2.1 Radiative loss

Next to the adiabatic temperature estimates, a useful characteristic number is the 'black body effective temperature'. Here, the approximation made is that the accretion energy is radiated

away from an optically thick surface of some geometry, under the assumption of a balance between the heating rate by release of accretion energy and cooling by radiation. For a specific example consider the surface of a star of radius R and mass M accreting via a disk. Most of the gravitational energy is released close to the star, in a region with surface area of the order, let's call it $4\pi R^2$. If the surface radiates approximately as a black body of temperature T (make a note of the fact that this is a bad approximation if the opacity is dominated by electron scattering), the balance would be

$$\dot{M} \frac{GM}{R} \approx 4\pi R^2 \sigma_r T^4, \quad (5)$$

where σ_r is the Stefan-Boltzmann constant, $\sigma_r = a_r c/4$ if a_r is Planck's radiation constant. For a neutron star with $M = 1.4M_\odot = 3 \cdot 10^{33}$ g, $R = 10$ km, accreting at a typical observed rate (near Eddington rate, see below), $\dot{M} = 10^{18}$ g/s $\approx 10^{-8}M_\odot/\text{yr}$, this temperature would be $T \approx 10^7$ K, or ≈ 1 keV per particle. Radiation with this characteristic temperature is observed in accreting neutron stars and black holes in their so-called 'soft X-ray states' (as opposed to their 'hard' states, in which the spectrum is very far from a black body).

The kinds of processes involved in radiation from accretion flows form a large subject in itself and will not be covered here. For introductions see Rybicki & Lightman (1979) and Frank et al. (2002). At the moderate temperatures encountered in protostars and white dwarf accreters, the dominant processes are the ones known from stellar physics: molecular and atomic transitions and Thomson scattering. Up to photon energies around 10 keV (the Lyman edge of an iron nucleus with one electron left) these processes also dominate the spectra of neutron star and black hole accreters. Above this energy, observed spectra become dominated by Compton scattering. Cyclotron/synchrotron radiation plays a role in when a strong magnetic field is present, which can happen in most classes of accreting objects.

2.3 Critical luminosity

Objects of high luminosity have a tendency to blow their atmospheres away due to the radiative force exerted when the outward traveling photons are scattered or absorbed. Consider a volume of gas on which a flux of photons is incident from one side. Per gram of matter, the gas presents a scattering (or absorbing) surface area of κ cm² to the escaping radiation. The force exerted by the radiative flux F on one gram is $F\kappa/c$. The force of gravity pulling back on this one gram of mass is GM/r^2 . The critical flux at which the two forces balance (energy per unit area and time) is

$$F_E = \frac{c}{\kappa} \frac{GM}{r^2}. \quad (6)$$

Assuming that this flux is *spherically symmetric*, it can be converted into a luminosity,

$$L_E = 4\pi GMc/\kappa, \quad (7)$$

the Eddington critical luminosity, popularly called the Eddington limit (e.g. Rybicki and Lightman, 1979). If the gas is fully ionized, its opacity is dominated by electron scatter-

ing, and for solar composition κ is then of the order $0.3 \text{ cm}^2/\text{g}$ (about a factor 2 lower for fully ionized helium). With these assumptions,

$$L_E \approx 1.7 \cdot 10^{38} \frac{M}{M_\odot} \text{ erg/s} \approx 4 \cdot 10^4 \frac{M}{M_\odot} L_\odot.$$

This number is different if the opacity is not dominated by electron scattering. In partially ionized gases of solar composition bound-bound and bound-free transitions can increase the opacity by a factor up to 10^3 ; the Eddington flux is then correspondingly lower.

If the luminosity results from accretion, one can define a corresponding Eddington characteristic accretion rate \dot{M}_E :

$$\frac{GM}{r} \dot{M}_E = L_E \quad \rightarrow \quad \dot{M}_E = 4\pi r c / \kappa. \quad (8)$$

With $\kappa = 0.3$:

$$\dot{M}_E \approx 1.3 \cdot 10^{18} r_6 \text{ g/s} \approx 2 \cdot 10^{-8} r_6 M_\odot \text{ yr}^{-1},$$

where r_6 is the radius of the accreting object in units of 10^6 cm . The characteristic accretion rate thus scales with the *size* of the accreting object, while the critical luminosity scales with *mass*.

Whereas L_E is a critical value which in several circumstances plays the role of a limit, the Eddington characteristic accretion rate is less of a limit. For more on exceptions to L_E and \dot{M}_E see 2.3.2 below.

2.3.1 Eddington luminosity at high optical depth

The Eddington characteristic luminosity was derived above under the assumption of a radiation flux passing through an optically thin medium surrounding the radiation source. What changes if the radiation passes through an optically thick medium, such as a stellar interior? At high optical depth the radiation field can be assumed to be nearly isotropic, and the *diffusion approximation* applies (cf. Rybicki & Lightman 1979). The radiative heat flux can then be written in terms of the radiation pressure P_r as

$$F_r = c \frac{dP_r}{d\tau}, \quad (9)$$

where τ is the optical depth

$$d\tau = \kappa \rho ds \quad (10)$$

along a path s , and κ an appropriate frequency-averaged opacity (such as the Rosseland mean). Balancing the gradient of the radiation pressure against the force of gravity gives the maximum radiation pressure that can be supported:

$$\nabla P_{r,\max} = \mathbf{g}\rho, \quad (11)$$

where \mathbf{g} is the acceleration of gravity. With (9) this yields the maximum radiation flux at a given point in a static gravitating object:

$$\mathbf{F}_{r,\max} = c\mathbf{g}/\kappa, \quad (12)$$

i.e. the same as the critical flux in the optically thin case.

2.3.2 Limitations of the Eddington limit

The derivation of F_E assumed that the force relevant in the argument is gravity. Other forces can be larger. An example would be a neutron star with a strong magnetic field. The curvature force $B^2/(4\pi r_c)$ in a loop of magnetic field (where r_c is the radius of curvature of the field lines) can balance a pressure gradient $\sim P/r_c$, so the maximum pressure that can be contained in a magnetic field¹ is of order $P \sim B^2/8\pi$. If the pressure is due to radiation, assuming an optical depth $\tau \geq 1$ so the diffusion approximation can be used, the maximum radiative energy flux is then of the order

$$F_{r,\max} \approx cP_r/\tau \approx c\frac{B^2}{8\pi\tau}. \quad (13)$$

In the range of validity of the assumptions made this has its maximum for an optical depth of order unity: $F_{r,\max} \approx cB^2/8\pi$. For a neutron star of radius $R = 10^6$ cm and a field strength of 10^{12} G, this gives $L_{r,\max} \approx 10^{46}$ erg/s, many orders of magnitude higher than the Eddington value L_E . [This explains the enormous luminosities that can be reached in so-called *magnetar outbursts*, e.g. Hurley et al. 2005].

The Eddington argument considers only the radiative flux. Larger energy fluxes are possible if energy is transported by other means, for example by convection.

Since L_E depends on opacity, it can happen that L_E is lower in the atmosphere of a star than in its interior. A luminous star radiating near its (internal) Eddington rate will then blow off its atmosphere in a *radiatively driven stellar wind*; this happens for example in Wolf-Rayet stars. In the context of protostellar accretion, the opacity in the star forming cloud from which the protostar accretes is high due to atomic and molecular transitions. As a result, the radiation pressure from a massive (proto-)star, with a luminosity approaching (2.3), is able to clear the away the molecular cloud from which it formed. This is believed to set a limit on the mass that can be reached by a star formed in a molecular cloud.

2.3.3 Neutron stars vs. black hole accreters

In deriving the critical accretion rate, it was assumed that the gravitational energy liberated is emitted in the form of radiation. In the case of a black hole accreter, this is not necessary since mass can flow through the hole's horizon, taking with it all energy contained in it. Instead of being emitted as radiation, the energy adds to the mass of the hole. This becomes especially important at high accretion rates, $\dot{M} > \dot{M}_E$ (and in the ion supported accretion flows

¹ Depending on circumstances the actual maximum is less than this because a magnetically contained plasma tends to 'leak across' field lines through MHD instabilities.

discussed in section 13). The parts of the flow close to the hole then become optically thick, the radiation stays trapped in the flow, and instead of producing luminosity gets swallowed by the hole. The accretion rate on a black hole can thus be arbitrarily large in principle (see also section 11, and chapter 10 in Frank et al, 2002).

A neutron star cannot absorb this much energy (only a negligible amount is taken up by conduction of heat into its interior), so \dot{M}_E is more relevant for neutron stars than for black holes. It is not clear to what extent it actually limits the possible accretion rate, however, since the limit was derived under the assumption of spherical symmetry. It is possible that accretion takes place in the form of an optically thick disk, while the energy released at the surface produces an outflow along the axis, increasing the maximum possible accretion rate (cf. discussion in 11). This has been proposed (e.g. King, 2004) as a possible conservative interpretation of the so-called ultraluminous X-ray sources (ULX), rare objects with luminosities of $10^{39} - 10^{41}$ erg/s. These are alternatively and more excitingly suggested to harbor intermediate mass black holes (above $\approx 30M_\odot$).

3 Accretion with Angular Momentum

When the accreting gas has a nonzero angular momentum with respect to the accreting object, it can not accrete directly. A new time scale then plays a role, the time scale for outward transport of angular momentum. Since this is in general much longer than the dynamical time scale, much of what was said about spherical accretion needs modification for accretion with angular momentum.

Consider the accretion in a close binary consisting of a compact (white dwarf, neutron star or black hole) primary of mass M_1 and a main sequence companion of mass M_2 . The mass ratio is defined as $q = M_2/M_1$ (note: in the literature q is just as often defined the other way around).

If M_1 and M_2 orbit each other in a circular orbit and their separation is a , the orbital frequency Ω is

$$\Omega^2 = G(M_1 + M_2)/a^3.$$

The accretion process is most easily described in a coordinate frame that corotates with this orbit, and with its origin in the center of mass. Matter that is stationary in this frame experiences an effective potential, the *Roche potential* (Ch. 4 in Frank, King and Raine, 2002), given by

$$\phi_R(\mathbf{r}) = -\frac{GM}{r_1} - \frac{GM}{r_2} - \frac{1}{2}\Omega^2\varpi^2 \quad (14)$$

where $r_{1,2}$ are the distances of point \mathbf{r} to stars 1,2, and ϖ the distance from the rotation axis (the axis through the center of mass, perpendicular to the orbit). Matter that does *not* corotate experiences a very different force (due to the Coriolis force). The Roche potential is therefore useful only in a rather limited sense. For non-corotating gas intuition based on the Roche geometry can be misleading. Keeping in mind this limitation, consider the equipotential surfaces of (14). The surfaces of stars $M_{1,2}$, assumed to corotate with the orbit, are equipotential surfaces of (14). Near the centers of mass (at low values of ϕ_R) they are unaffected by the

other star, at higher Φ they are distorted and at a critical value Φ_1 the two parts of the surface touch. This is the critical Roche surface S_1 whose two parts are called the Roche lobes.

Binaries lose angular momentum through gravitational radiation and a magnetic wind from the secondary (if it has a convective envelope). Through this loss the separation between the components decreases and both Roche lobes decrease in size. Mass transfer starts when M_2 fills its Roche lobe, and continues as long as the angular momentum loss from the system lasts. Mass transfer can also be due to expansion of the secondary in course of its evolution, and mass transfer can be a runaway process, depending on mass and internal structure of the secondary. This is a classical subject in the theory of binary stars, for an introduction see Warner (1995).

A stream of gas then flows through the point of contact of the two parts of S_1 , the inner Lagrange point L_1 . If the force acting on it were derivable entirely from (14) the gas would just fall in radially onto M_1 . As soon as it moves however, it does not corotate any more and its orbit under the influence of the Coriolis force is different (Fig. 1).

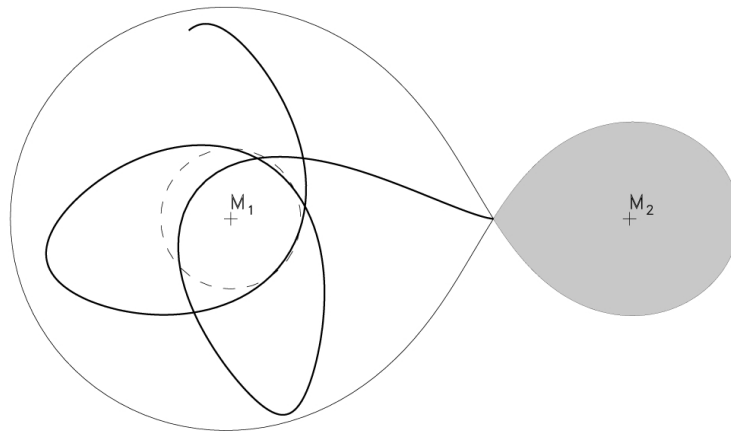


Fig. 1 Roche geometry for $q = 0.2$, with free particle orbit from L_1 (as seen in a frame corotating with the orbit). Dashed: circularization radius.

Since the gas at L_1 is usually very cold compared with the virial temperature, the velocity it acquires exceeds the sound speed already after moving a small distance from L_1 . The flow into the Roche lobe of M_1 is therefore highly *supersonic*. Such hypersonic flow is essentially ballistic, that is, the stream flows approximately along the path taken by freely falling particles.

Though the gas stream on the whole follows a path close to that of a free particle, a strong shock develops at the point where the path intersects itself². After this, the gas settles into a ring, into which the stream continues to feed mass. If the mass ratio q is not too small this ring

² In practice shocks already develop shortly after passing the pericenter at M_1 , when the gas is decelerated again. Supersonic flows that are decelerated, by whatever means, in general develop shocks (e.g. Courant and Friedrichs 1948, Massey, 1968). The effect can be seen in action in the movie published in Różyczka and Spruit, 1993.

forms fairly close to M_1 . An approximate value for its radius is found by noting that near M_1 the tidal force due to the secondary is small, so that the angular momentum of the gas with respect to M_1 is approximately conserved. If the gas continues to conserve angular momentum while dissipating energy, it settles into the minimum energy orbit with the specific angular momentum j of the incoming stream. The value of j is found by a simple integration of the orbit starting at L_1 and measuring j at some point near pericenter. The radius of the orbit, the nominal *circularization radius* r_c is then defined through $(GM_1 r_c)^{1/2} = j$. In units of the orbital separation a , r_c and the distance r_{L1} from M_1 to L_1 are functions of the mass ratio only. As an example for $q = 0.2$, $r_{L1} \approx 0.66a$ and the circularization radius $r_c \approx 0.16a$. In practice the ring forms somewhat outside r_c , because there is some angular momentum redistribution in the shocks that form at the impact of the stream on the ring. The evolution of the ring depends critically on nature and strength of the angular momentum transport processes. If sufficient ‘viscosity’ is present it spreads inward and outward to form a disk.

At the point of impact of the stream on the disk the energy dissipated is a significant fraction of the orbital kinetic energy, hence the gas heats up to a significant fraction of the virial temperature. For a typical system with $M_1 = 1M_\odot$, $M_2 = 0.2M_\odot$ and an orbital period of 2 hrs, the observed size of the disk (e.g. Wood et al. 1989b, Rutten et al. 1992) $r_d/a \approx 0.3$, the orbital velocity at r_d about 900 km/s, and the virial temperature at r_d is $\approx 10^8$ K. The actual temperatures at the impact point are much lower, due to rapid cooling of the shocked gas. Nevertheless the impact gives rise to a prominent ‘hot spot’ in many systems, and an overall heating of the outermost part of the disk.

4 Thin disks: properties

4.1 Flow in a cool disk is supersonic

Ignoring viscosity, the equation of motion in the potential of a point mass is

$$\frac{\partial \mathbf{v}}{\partial t} + \mathbf{v} \cdot \nabla \mathbf{v} = -\frac{1}{\rho} \nabla P - \frac{GM}{r^2} \hat{\mathbf{r}}, \quad (15)$$

where $\hat{\mathbf{r}}$ is a unit vector in the spherical radial direction r . To compare the order of magnitude of the terms, choose a position r_0 in the disk, and choose as typical time and velocity scales the orbital time scale $\Omega_0^{-1} = (r_0^3/GM)^{1/2}$ and velocity $\Omega_0 r_0$. For simplicity of the argument, assume a fixed temperature T . The pressure gradient term is then

$$\frac{1}{\rho} \nabla P = \frac{\mathcal{R}}{\mu} T \nabla \ln P.$$

In terms of the dimensionless quantities

$$\begin{aligned} \tilde{r} &= r/r_0, & \tilde{v} &= v/(\Omega_0 r_0), \\ \tilde{t} &= \Omega_0 t, & \tilde{\nabla} &= r_0 \nabla, \end{aligned}$$

the equation of motion becomes

$$\frac{\partial \tilde{\mathbf{v}}}{\partial \tilde{t}} + \tilde{\mathbf{v}} \cdot \tilde{\nabla} \tilde{\mathbf{v}} = -\frac{T}{T_{\text{vir}}} \tilde{\nabla} \ln P - \frac{1}{\tilde{r}^2} \hat{\mathbf{r}}. \quad (16)$$

All terms and quantities in this equation are of order unity by the assumptions made, except the pressure gradient term which has the coefficient T/T_{vir} in front. If cooling is important, so that $T/T_{\text{vir}} \ll 1$, the pressure term is negligible to first approximation. Equivalent statements are also that the gas moves hypersonically on nearly Keplerian orbits, and that the disk is thin, as is shown next.

4.2 Disk thickness

The thickness of the disk is found by considering its equilibrium in the direction perpendicular to the disk plane. In an axisymmetric disk, using cylindrical coordinates (ϖ, ϕ, z) , consider the forces at a point $\mathbf{r}_0(\varpi, \phi, 0)$ in the midplane, in a frame rotating with the Kepler rate Ω_0 at that point. The gravitational acceleration $-GM/r^2 \hat{\mathbf{r}}$ balances the centrifugal acceleration $\Omega_0^2 \hat{\boldsymbol{\omega}}$ at this point, but not at some distance z above it because gravity and centrifugal acceleration work in different directions. Expanding both accelerations near \mathbf{r}_0 , one finds a residual acceleration toward the midplane of magnitude

$$g_z = -\Omega_0^2 z.$$

Assuming an isothermal gas at temperature T , the condition for equilibrium in the z -direction under this acceleration yields a hydrostatic density distribution

$$\rho = \rho_0(\varpi) \exp\left(-\frac{z^2}{2H^2}\right).$$

$H(\varpi)$, called the *scale height* of the disk or simply the disk thickness, is given in terms of the isothermal sound speed $c_i = (\mathcal{R}T/\mu)^{1/2}$ by

$$H = c_i/\Omega_0. \quad (17)$$

Define $\delta \equiv H/r$, the *aspect ratio* of the disk; it can be expressed in several equivalent ways:

$$\delta = \frac{H}{r} = \frac{c_i}{\Omega r} = \frac{1}{\text{Ma}} = \left(\frac{T}{T_{\text{vir}}}\right)^{1/2}, \quad (18)$$

where Ma is the Mach number of the orbital motion.

4.3 Viscous spreading

The shear flow between neighboring Kepler orbits in the disk causes friction if some form of viscosity is present. The frictional torque is equivalent to exchange of angular momentum between these orbits. But since the orbits are close to Keplerian, a change in angular momentum of a ring of gas also means it must change its distance from the central mass. If the angular momentum is increased, the ring moves to a larger radius. In a thin disk angular momentum transport (more precisely a nonzero divergence of the angular momentum flux) therefore automatically implies redistribution of mass in the disk.

A simple example (Lüst 1952, see also Lynden-Bell and Pringle 1974) is a narrow ring of gas at some distance r_0 . If at $t = 0$ this ring is released to evolve under the viscous torques, one finds that it first spreads into an asymmetric hump. The hump quickly spreads inward onto the central object while a long tail spreads slowly outwards to large distances. As $t \rightarrow \infty$ almost all the *mass* of the ring accretes onto the center, while a vanishingly small fraction of the gas carries almost all the *angular momentum* to infinity.

As a result of this asymmetric behavior essentially all the mass of a disk can accrete even if the total angular momentum of the disk is conserved. In practice, however, there is often an external torque removing angular momentum from the disk: when the disk results from mass transfer in a binary system. The tidal forces exerted by the companion star take up angular momentum from the outer parts of the disk, limiting its outward spreading.

4.4 Observational evidence of disk viscosity

Evidence for the strength of the angular momentum transport processes in disks comes from observations of variability time scales. This evidence is not good enough to determine whether the processes really behave in the same way as viscosity, but if this is assumed, estimates can be made of its magnitude.

Observations of Cataclysmic Variables (CV) give the most detailed information. These are binaries with white dwarf (WD) primaries and (usually) main sequence companions (for reviews see Meyer-Hofmeister and Ritter 1993, 1995, Warner 1995). A subclass of these systems, the Dwarf Novae, show semiregular outbursts. In the currently most developed theory, these outbursts are due to an instability in the disk (Smak 1971, Meyer and Meyer-Hofmeister 1981, King 1995, Hameury et al. 1998). The outbursts are episodes of enhanced accretion of mass from the disk onto the primary, involving a significant part of the whole disk. The decay time of the burst is thus a measure of the viscous time scale of the disk (the quantitative details depend on the model, see Cannizzo et al. 1988, Hameury et al. 1998):

$$t_{\text{visc}} = r_d^2/\nu,$$

where r_d is the size of the disk, $\sim 10^{10}$ cm for a CV. With decay times on the order of days, this yields viscosities of the order 10^{15} cm²/s, some 14 orders of magnitude above the microscopic ('molecular') viscosity of the gas.

Other evidence comes from the inferred time scale on which disks around protostars disappear, which is of the order of 10^7 years (e.g. Strom et al., 1993).

4.5 α -parameterization

Several processes have been proposed to account for these short time scales and the large apparent viscosities inferred from them. One of these is that accretion does not in fact take place through a viscous-like process as described above at all, but results from angular momentum loss through a magnetic wind driven from the disk surface (Bisnovatyi-Kogan & Ruzmaikin 1976, Blandford 1976), much in the way sun-like stars spin down by angular momentum loss through their stellar winds. The extent to which this plays a role in accretion disks is still uncertain. It would be a ‘quiet’ form of accretion, since it can do without energy dissipating processes like viscosity. It has been proposed as the explanation for the low ratio of X-ray luminosity to jet power in many radio sources (see Migliari and Fender 2006 and references therein). This low ratio, however, is also plausibly attributed to the low efficiency with which X-rays are produced in the ‘ion supported accretion flows’ (see section 13 below) which are expected to be the source of the jet outflows observed from X-ray binaries and AGN.

The most quantitatively developed mechanism for angular momentum transport is a form of magnetic viscosity (anticipated already in Shakura and Sunyaev 1973). This is discussed below in section 8.1. It requires the accreting plasma to be sufficiently electrically conducting. This is often the case, but not always: it is questionable for example in the cool outer parts of protostellar disks. Other mechanisms thus still play a role in the discussion, for example spiral shocks (Spruit et al. 1987) and self-gravitating instabilities (Paczynski 1978, Gammie 1997).

In order to compare the viscosities of disks in objects with (widely) different sizes and physical conditions, introduce a dimensionless viscosity α :

$$\nu = \alpha \frac{c_1^2}{\Omega}, \quad (19)$$

where c_1 is the isothermal sound speed as before. The quantity α was introduced by Shakura and Sunyaev (1973) as a way of parametrizing our ignorance of the angular momentum transport process, in a way that allows comparison between systems of very different size and physical origin (Their definition of α differs a bit, by a constant factor of order unity).

4.6 Causality limit on turbulent viscosity

How large can the value of α be, on theoretical grounds? As a simple model, let’s assume that the shear flow between Kepler orbits is unstable to the same kind of shear instabilities found for flows in tubes, channels, near walls and in jets. These instabilities occur so ubiquitously that the fluid mechanics community considers them an automatic consequence of a high Reynolds number:

$$Re = \frac{LV}{\nu}$$

where L and V are characteristic length and velocity scales of the flow. If this number exceeds about 1000 (for some forms of instability much less), instability and turbulence are generally observed. It has been argued (e.g. Zel'dovich 1981) that for this reason hydrodynamic turbulence is the cause of disk viscosity. Let's look at the consequences of this assumption. If an eddy of radial length scale l develops due to shear instability, it will rotate at a rate given by the rate of shear in the flow, σ , in a Keplerian disk

$$\sigma \approx r \frac{\partial \Omega}{\partial r} = -\frac{3}{2} \Omega.$$

The velocity amplitude of the eddy is $V = \sigma l$, and a field of such eddies would produce a turbulent viscosity of the order (leaving out numerical factors of order unity)

$$\nu_{\text{turb}} \approx l^2 \Omega. \quad (20)$$

In compressible flows, there is a maximum to the size of the eddy set by causality considerations. The force that allows an instability to form a coherently overturning eddy is the pressure, which transports information about the flow at the speed of sound. The eddies formed by a shear instability can therefore not rotate faster than c_i , hence their size does not exceed $c_i/\sigma \approx H$ (eq. 18). At the same time, the largest eddies formed also have the largest contribution to the exchange of angular momentum. Thus we should expect that the turbulent viscosity is given by eddies with size of the order H :

$$\nu < H^2 \Omega,$$

or

$$\alpha < 1.$$

The dimensionless number α can thus be interpreted as the effective viscosity in units of the maximum value expected if a disk were hydrodynamically turbulent.

4.6.1 Large scale vortices?

The small size of hydrodynamic eddies expected, $L < H = c_i/\Omega$, is due to the high Mach number of the flow in an accretion disk; this makes a disk behave like a very *compressible* fluid. Attempts to construct large scale vortices $L \gg H$ in disks using *incompressible* fluid analogies continue to be made, both analytically and experimentally. Expansions in disk thickness as a small parameter then suggest themselves, in analogy with large scale flows such as weather systems and tropical storms in the Earth's atmosphere. The size of these systems is large compared with the height of the Earth's atmosphere, and expansions making use of this can be effective. This tempting analogy is misleading for accretion disks, however, since in contrast with the atmosphere all flows with a horizontal scale exceeding the vertical thickness are supersonic, and the use of incompressible fluid models meaningless.

4.7 Hydrodynamic turbulence?

Does hydrodynamical turbulence along these lines actually exist in disks? In the astrophysical community, a consensus has developed that it does *not*, certainly not along the simple lines suggested by a Reynolds' number argument. An intuitive argument is that the flow in a cool disk is close to Kepler orbits, and these are quite stable. Numerical simulations of disk-like flows with different rotation profiles do not show the expected shear flow instabilities in cases where the angular momentum increases outward, while turbulence put in by hand as initial condition decays in such simulations (Hawley et al. 1999).

Analytical work on the problem has not been able to demonstrate instability in this case either (for recent work and references see Lesur & Longaretti 2005, Rincon et al. 2007). Existing proposals for disk turbulence involve ad-hoc assumptions about the existence of hydrodynamic instabilities (e.g. Dubrulle 1992). However, a subtle form of hydrodynamic angular momentum transport has been identified more recently (Lesur & Papaloizou 2010); it depends on vertical stratification of the disk as well as the presence of a convectively unstable *radial* gradient.

A laboratory analogy is the rotating Couette flow, an experiment with water between differentially rotating cylinders. Recent such experiments have demonstrated that turbulence is absent in cases where angular momentum increases outward (as in Keplerian rotation) at Reynolds' numbers as high as 10^6 (the Princeton Couette experiment, Ji et al. 2006).

In view of these negative results, the popular mechanism for angular momentum transport in accretion disk has become magnetic: 'MRI turbulence' (section 8.1). But beware: in the fluid mechanics community it is considered crackpot to suggest that at Reynolds numbers like our 10^{14} a flow (no matter which or where) can be anything but 'fiercely turbulent'. If your career depends on being friends with this community, it would be wise to avoid discussions about accretion disks or Couette experiments.

5 Thin Disks: equations

Consider a thin (= cool, nearly Keplerian, cf. section 4.2) disk, axisymmetric but not stationary. Using cylindrical coordinates (r, ϕ, z) , (note that we have changed notation from ϖ to r compared with 4.2) we define the *surface density* Σ of the disk as

$$\Sigma = \int_{-\infty}^{\infty} \rho dz \approx 2H_0\rho_0, \quad (21)$$

where ρ_0, H_0 are the density and scaleheight at the midplane. The approximate sign is used to indicate that the coefficient in front of H in the last expression actually depends on details of the vertical structure of the disk. Conservation of mass, in terms of Σ is described by

$$\frac{\partial}{\partial t}(r\Sigma) + \frac{\partial}{\partial r}(r\Sigma v_r) = 0. \quad (22)$$

(derived by integrating the continuity equation over z). Since the disk is axisymmetric and nearly Keplerian, the radial equation of motion reduces to

$$v_\phi^2 = GM/r. \quad (23)$$

The ϕ -equation of motion is

$$\frac{\partial v_\phi}{\partial t} + v_r \frac{\partial v_\phi}{\partial r} + \frac{v_r v_\phi}{r} = F_\phi, \quad (24)$$

where F_ϕ is the azimuthal component of the viscous force. By integrating this over height z and using (22), one gets an equation for the angular momentum balance:

$$\frac{\partial}{\partial t}(r\Sigma\Omega r^2) + \frac{\partial}{\partial r}(r\Sigma v_r \Omega r^2) = \frac{\partial}{\partial r}(S r^3 \frac{\partial \Omega}{\partial r}), \quad (25)$$

where $\Omega = v_\phi/r$, and

$$S = \int_{-\infty}^{\infty} \rho v dz \approx \Sigma v. \quad (26)$$

The second approximate equality in (26) holds if v can be considered independent of z . The right hand side of (25) is the divergence of the viscous angular momentum flux, and is derived most easily with a physical argument, as described in, e.g. Pringle (1981) or Frank et al. (2002)³.

Assume now that v can be taken constant with height. For an isothermal disk (T independent of z), this is equivalent to taking the viscosity parameter α independent of z . As long as we are not sure what causes the viscosity this is a reasonable simplification. Note, however, that recent numerical simulations of magnetic turbulence suggest that the effective α , and the rate of viscous dissipation per unit mass, are higher near the disk surface than near the midplane (c.f. section 8). While eq. (25) is still valid for rotation rates Ω deviating from Keplerian (only the integration over disk thickness must be justifiable), we now use the fact that $\Omega \sim r^{-3/2}$. Then eqs. (22-25) can be combined into a single equation for Σ :

$$r \frac{\partial \Sigma}{\partial t} = 3 \frac{\partial}{\partial r} [r^{1/2} \frac{\partial}{\partial r} (v \Sigma r^{1/2})]. \quad (27)$$

Under the same assumptions, eq. (24) yields the mass flux \dot{M} at any point in the disk:

³ If you prefer a more formal derivation, the fastest way is to consult Landau and Lifshitz (1959) chapter 15 (hereafter LL). Noting that the divergence of the flow vanishes for a thin axisymmetric disk, the viscous stress σ becomes (LL eq. 15.3)

$$\sigma_{ik} = \eta \left(\frac{\partial v_i}{\partial x_k} + \frac{\partial v_k}{\partial x_i} \right),$$

where $\eta = \rho v$. This can be written in cylindrical or spherical coordinates using LL eqs. (15.15-15.18). The viscous force is

$$F_i = \frac{\partial \sigma_{ik}}{\partial x_k} = \frac{1}{\eta} \frac{\partial \eta}{\partial x_k} \sigma_{ik} + \eta \nabla^2 v_i,$$

Writing the Laplacian in cylindrical coordinates, the viscous torque is then computed from the ϕ -component of the viscous force by multiplying by r , and is then integrated over z .

$$\dot{M} = -2\pi r \Sigma v_r = 6\pi r^{1/2} \frac{\partial}{\partial r} (v \Sigma r^{1/2}). \quad (28)$$

Eq. (27) is the standard form of the *thin disk diffusion equation*. An important conclusion from this equation is: in the thin disk limit, all the physics which influences the time dependent behavior of the disk enters through one quantity only: the viscosity ν . This is the main attraction of the thin disk approximation.

5.1 Steady thin disks

In a steady disk ($\partial/\partial t = 0$) the mass flux \dot{M} is constant through the disk and equal to the accretion rate onto the central object. From (28) we get the surface density distribution:

$$v \Sigma = \frac{1}{3\pi} \dot{M} \left[1 - \beta \left(\frac{r_i}{r} \right)^{1/2} \right], \quad (29)$$

where r_i is the inner radius of the disk and β is a parameter appearing through the integration constant. It is related to the flux of angular momentum F_J through the disk:

$$F_J = -\dot{M} \beta \Omega_i r_i^2, \quad (30)$$

where Ω_i is the Kepler rotation rate at the inner edge of the disk. If the disk accretes onto an object with a rotation rate Ω_* less than Ω_i , the rotation rate $\Omega(r)$ as a function of distance r jumps from Ω_* close to the star to the Kepler rate $\Omega_K(r)$ in the disk. It then has a maximum at some distance close to the star (distance of the order of the disk thickness H). At this point the viscous stress (proportional to $\partial_r \Omega$) vanishes and the angular momentum flux is just the amount carried by the accretion flow. In (30) this corresponds to $\beta = 1$, *independent* of Ω_* (Shakura and Sunyaev, 1973, Lynden-Bell and Pringle, 1974). This is referred to as the standard or ‘accreting case’. The angular momentum flux (equal to the torque on the accreting star), is then inward, causing the rotation rate of the star to increase (spinup).

For stars rotating near their maximum rate ($\Omega_* \approx \Omega_i$) and for accretion onto magnetospheres, which can rotate faster than the disk, the situation is different (Sunyaev and Shakura 1977, Popham and Narayan 1991, Paczyński 1991, Bisnovatyi-Kogan 1993, Rappaport et al. 2004). If the inner edge of the disk is at the *corotation radius* r_{co} , defined by

$$\Omega_K(r_{co}) = \Omega_*, \quad (31)$$

the viscous stress cannot be assumed to vanish there, and the thin disk approximation does not give a unique answer for the angular momentum flux parameter β . Its value is then determined by details of the hydrodynamics at r_{co} , which need to be investigated separately. Depending on the outcome of this investigation, values varying from 1 (spinup, standard accreting case) to negative values (spindown) are possible. As (30) shows, the surface density at the inner edge of the disk depends sensitively on the value of β (see also Fig. 2). This plays a role in the cyclic accretion process discussed in the next subsection.

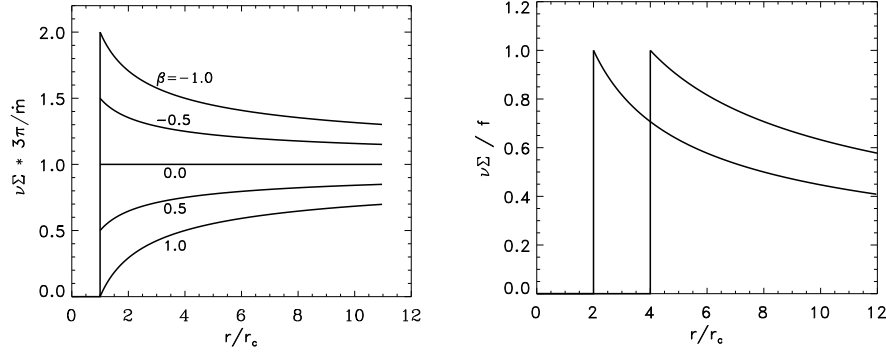


Fig. 2 Surface density $\nu\Sigma$ of a thin disc as a function of distance from the corotation radius r_c , for a steady, thin viscous disc. Left: steady accretion at a fixed accretion rate \dot{m} , for inner edge of the disc at corotation. β measures the angular momentum flux, $\beta = -1$ corresponding to the standard case of accretion on to a slowly rotation object. For $\beta < 0$ the angular momentum flux is outward (spindown of the star). Right: ‘quiescent disc’ solutions with $\dot{m} = 0$ and a steady outward angular momentum flux due to a torque f applied at the inner edge.

5.2 Magnetospheres, ‘propellering’ and ‘dead disks’

Stars with magnetospheres, instead of spinning up by accretion of angular momentum from the disk, can actually *spin down* by interaction with the disk, even while accretion is still going on. The thin disk approximation above covers this case as well (cf. figure 2). The surface density distribution is then of the form (29), but with $\beta < 0$ (see also Spruit and Taam 1993, Rappaport et al. 2004). The angular momentum flux through the disk is outward, and the accreting star spins down. This is possible even when the interaction between the disk and the magnetosphere takes place *only* at the inner edge of the disk. Magnetic torques due interaction between the disk and the magnetosphere may exist at larger distances in the disk as well, but are not necessary for creating an outward angular momentum flux. Numerical simulations of disk-magnetosphere interaction (Miller and Stone 1997, for recent work see Long et al. 2008 and references therein) give an interesting view of how such interaction may take place, presenting a picture that is very differently from what is assumed in the previous ‘standard’ models. Among other things, they show the interaction region to be quite narrow.

Rapidly rotating magnetospheres play a role in some CVs and X-ray binaries, and probably also in protostellar accretion disks. When the rotation velocity of the magnetosphere is larger than the Kepler velocity at the inner edge of the disk (i.e. when $r_1 > r_{co}$), the literature often assumes that the mass transferred from the secondary must be ‘flung out’ of the binary system. This idea is called ‘propellering’ (Illarionov and Sunyaev 1975). The term is then used as synonymous with the condition $r_1 > r_{co}$. While a process like this is likely to happen when the rotation rate of the star is sufficiently large (the CV AE Aqr being an example) it is not necessary. It is not possible either, when the difference in rotation velocity is too small to put the accreting mass on an escape orbit. This has been realized early on (Sunyaev and Shakura 1977). Instead of being flung out, accretion is halted and mass accumulates in the disk. The buildup of mass in the disk then leads to a following episode of accretion. In this phase the

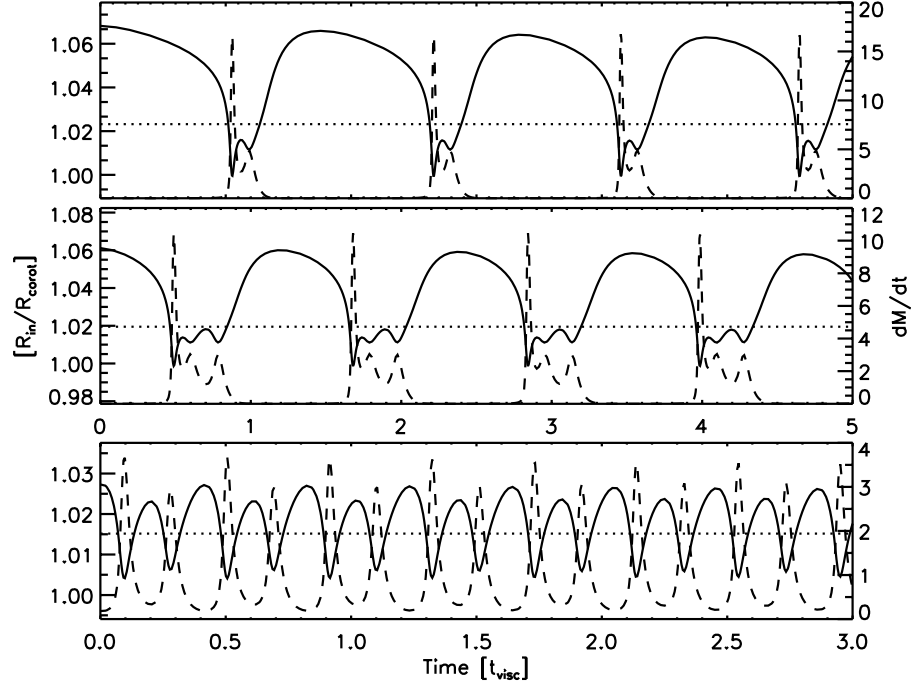


Fig. 3 Cyclic accretion due to interaction between a magnetosphere and a disk with inner edge near corotation. Solid: inner edge radius of the disk in units of the corotation radius; dashed: accretion rate (from D’Angelo and Spruit 2010).

magnetosphere is compressed such that $r_i < r_{co}$. Instead of propelling, the result is *cyclic* accretion. For quantitative models see D’Angelo and Spruit (2010), an example is shown in Figure 3. The phase with $r_i > r_{co}$, during which accretion is halted is called ‘dead disk’ phase in Sunyaev and Shakura (1977).

5.3 Disk Temperature

In this section I assume accretion onto not-too-rapidly rotating objects, so that $\beta = 1$ (eq. 29). The surface temperature of the disk, which determines how much energy it loses by radiation, is governed by the energy dissipation rate in the disk, which in turn is given by the accretion rate. From the first law of thermodynamics we have

$$\rho T \frac{dS}{dt} = -\text{div}\mathbf{F} + Q_v, \quad (32)$$

where S is the entropy per unit mass, \mathbf{F} the heat flux (including radiation and convection), and Q_v the viscous dissipation rate. For thin disks, where the advection of internal energy

(or entropy) can be neglected, and for changes which happen on time scales longer than the dynamical time Ω^{-1} , the left hand side is small compared with the terms on the right hand side. Integrating over z , the divergence turns into a surface term and we get

$$2\sigma_r T_s^4 = \int_{-\infty}^{\infty} Q_v dz, \quad (33)$$

where T_s is the surface temperature of the disk, σ_r is Stefan-Boltzmann's radiation constant $\sigma_r = a_r c/4$, and the factor 2 comes about because the disk has 2 radiating surfaces (assumed to radiate like black bodies). Thus the energy balance is *local* (for such slow changes): what is generated by viscous dissipation inside the disk at any radius r is also radiated away from the surface at that position. The viscous dissipation rate is equal to $Q_v = \sigma_{ij} \partial v_i / \partial x_j$, where σ_{ij} is the viscous stress tensor (see footnote in section 5), and this works out⁴ to be

$$Q_v = 9/4 \Omega^2 \nu \rho. \quad (34)$$

Eq. (33), using (29) then gives the surface temperature in terms of the accretion rate:

$$\sigma_r T_s^4 = \frac{9}{8} \Omega^2 \nu \Sigma = \frac{GM}{r^3} \frac{3\dot{M}}{8\pi} \left[1 - \left(\frac{r_i}{r} \right)^{1/2} \right]. \quad (35)$$

This shows that the surface temperature of the disk, at a given distance r from a steady accreter, depends *only* on the product $M\dot{M}$, and not on the highly uncertain value of the viscosity. For $r \gg r_i$ we have

$$T_s \sim r^{-3/4}. \quad (36)$$

These considerations only tells us about the surface temperature. The internal temperature in the disk is quite different, and depends on the mechanism transporting energy to the surface. Because it is the internal temperature that determines the disk thickness H (and probably also the viscosity), this transport needs to be considered in some detail for realistic disk models. This involves a calculation of the vertical structure of the disk. Because of the local (in r) nature of the balance between dissipation and energy loss, such calculations can be done as a grid of models in r , without having to deal with exchange of energy between neighboring models. Schemes borrowed from stellar structure computations are used (e.g. Meyer and Meyer-Hofmeister 1982, Cannizzo et al. 1988).

An approximation to the temperature in the disk can be found when a number of additional assumptions is made. As in stellar interiors, the energy transport is radiative rather than convective at high temperatures. Assuming local thermodynamic equilibrium (LTE, e.g. Rybicki and Lightman 1979), the temperature structure of a radiative atmosphere is given, in the so-called Eddington approximation of radiative transfer (not to be confused with the Eddington limit) by:

$$\frac{d}{d\tau} \sigma_r T^4 = \frac{3}{4} F. \quad (37)$$

The boundary condition that there is no incident flux from outside the atmosphere yields the approximate condition

⁴ using, e.g. LL eq. 16.3

$$\sigma_r T^4(\tau = 2/3) = F, \quad (38)$$

where $\tau = \int_z^\infty \kappa \rho dz$ is the optical depth at geometrical depth z , and F the energy flux through the atmosphere. Assuming that most of the heat is generated near the midplane (which is the case if ν is constant with height), F is approximately constant with height and equal to $\sigma_r T_s^4$, given by (35). Eq (37) then yields

$$\sigma_r T^4 = \frac{3}{4} \left(\tau + \frac{2}{3} \right) F. \quad (39)$$

Approximating the opacity κ as constant with z , the optical depth at the midplane is $\tau = \kappa \Sigma / 2$. If $\tau \gg 1$, the temperature at the midplane is then:

$$T^4 = \frac{27}{64} \sigma_r^{-1} \Omega^2 \nu \Sigma^2 \kappa. \quad (40)$$

With the equation of state (2), valid when radiation pressure is small, we find for the disk thickness, using (29):

$$\begin{aligned} \frac{H}{r} &= (\mathcal{R}/\mu)^{2/5} (\sigma_r 64 / 3 \pi^2)^{-1/10} (\kappa/\alpha)^{1/10} (GM)^{-7/20} r^{1/20} (f\dot{M})^{1/5} \\ &= 5 \cdot 10^{-3} \alpha^{-1/10} r_6^{1/20} (M/M_\odot)^{-7/20} (f\dot{M}_{16})^{1/5}, \quad (P_r \ll P) \end{aligned} \quad (41)$$

where $r_6 = r/(10^6 \text{ cm})$, $\dot{M}_{16} = \dot{M}/(10^{16} \text{ g/s})$, and

$$f = 1 - (r_i/r)^{1/2}.$$

From this we conclude: i) that the disk is thin in X-ray binaries, $H/r < 0.01$, ii) the disk thickness is relatively insensitive to the parameters, especially α , κ and r . It must be stressed, however, that this depends fairly strongly on the assumption that the energy is dissipated in the disk interior. If the dissipation takes place close to the surface, such as in some magnetic reconnection models, the internal disk temperature will be much closer to the surface temperature (Haardt et al. 1994, Di Matteo et al. 1999a and references therein). The midplane temperature and H are even smaller in such disks than calculated from (41).

5.4 A subtlety: viscous vs. gravitational energy release

The viscous dissipation rate per unit area of the disk, $W_v = (9/4)\Omega^2 \nu \Sigma$ [cf. eq. 35)] can be compared with the local rate W_G at which gravitational energy is liberated in the accretion flow. Since half the gravitational energy stays in the flow as orbital motion, we have

$$W_G = \frac{1}{2\pi r} \frac{GM\dot{M}}{2r^2}, \quad (42)$$

so that, in a steady thin disk accreting on a slowly rotating object (using eq. 29):

$$W_v/W_G = 3f = 3[1 - (r_i/r)^{1/2}]. \quad (43)$$

At large distances from the inner edge, the dissipation rate is *3 times larger than the rate of gravitational energy release*. This may seem odd, but becomes understandable when it is realized that there is a significant flux of energy through the disk associated with the viscous stress⁵. Integrating the viscous energy dissipation over the whole disk, one finds

$$\int_{r_i}^{\infty} 2\pi r W_v dr = \frac{GM\dot{M}}{2r_i}, \quad (44)$$

as expected. That is, globally but not locally, half of the gravitational energy is radiated from the disk while the other half remains in the orbital kinetic energy of the material accreting on the star.

What happens to this remaining orbital energy depends on the nature of the accreting object. If the object is a slowly rotating black hole, the orbital energy is just swallowed by the hole. If it has a solid surface, the orbiting gas slows down until it corotates with the surface, dissipating the orbital energy into heat in a boundary layer. Unless the surface rotates close to the orbital rate ('breakup'), the energy released in this way is of the same order as the total energy released in the accretion disk. The properties of this boundary layer are therefore critical for accretion onto neutron stars and white dwarfs. See also section 9.1 and Inogamov and Sunyaev (1999).

5.5 Radiation pressure dominated disks

In the inner regions of disks in XRB, the radiation pressure can dominate over the gas pressure, which results in a different expression for the disk thickness. The total pressure P is

$$P = P_r + P_g = \frac{1}{3}aT^4 + P_g. \quad (45)$$

Defining a 'total sound speed' by $c_t^2 = P/\rho$ the relation between temperature and disk thickness (17) still holds, so $c_t = \Omega H$. For $P_r \gg P_g$ we get from (40), with (35) and $\tau \gg 1$:

$$cH = \frac{3}{8\pi} \kappa f \dot{M},$$

(where the rather approximate relation $\Sigma = 2H\rho_0$ has been used). Thus,

$$\frac{H}{R} \approx \frac{3}{8\pi} \frac{\kappa}{cR} f \dot{M} = \frac{3}{2} f \frac{\dot{M}}{\dot{M}_E}, \quad (46)$$

where R is the stellar radius and \dot{M}_E the Eddington rate for this radius. It follows that the disk becomes thick near the star, if the accretion rate is near Eddington (though this is mitigated

⁵ See Landau & Lifshitz section 16

somewhat by the factor f). Accretion near the Eddington limit is evidently not geometrically thin any more. In addition, other processes such as angular momentum loss from the disk by ‘photon drag’ in the dense radiation field of the accreting star have to be taken into account.

6 Time scales in thin disks

A number of time scales play a role in the behavior of disks. In a thin disk they differ by powers of the large factor r/H . The shortest of these is the dynamical time scale t_d :

$$t_d = \Omega K^{-1} = (GM/r^3)^{-1/2}. \quad (47)$$

The time scale for radial drift through the disk over a distance of order r is the viscous time scale:

$$t_v = r/(-v_r) = \frac{2}{3} \frac{rf}{v} = \frac{2f}{3\alpha\Omega} \left(\frac{r}{H}\right)^2, \quad (48)$$

(using (28) and (29), valid for steady accretion). This is of the order $(r/H)^2$ longer than the dynamical time scale, except near the inner edge of the disk, where $f \downarrow 0$, and this time scale formally drops to zero as a consequence of the thin disk approximations. If more physics were included, the viscous time scale would stay above the dynamical time scale.

Intermediate are *thermal* time scales. If E_t is the thermal energy content (enthalpy) of the disk per unit of surface area, and $W_v = (9/4)\Omega^2 v \Sigma$ the heating rate by viscous dissipation, we can define a heating time scale:

$$t_h = E_t/W_v. \quad (49)$$

In the same way, a cooling time scale is defined by the energy content and the radiative loss rate:

$$t_c = E_t/(2\sigma_r T_s^4). \quad (50)$$

For a thin disk, the two are equal since the viscous energy dissipation is locally balanced by radiation from the two disk surfaces. [In thick disks (ADAFs), this balance does not hold, since the advection of heat with the accretion flow is not negligible. In this case $t_c > t_h$ (see section 12)]. Thus, we can replace both time scales by a single thermal time scale t_t , and find, with (34):

$$t_t = \frac{1}{W_v} \int_{-\infty}^{\infty} \frac{\gamma P}{\gamma - 1} dz, \quad (51)$$

where the enthalpy of an ideal gas of constant ratio of specific heats γ has been used. Leaving out numerical factors of order unity, this yields

$$t_t \approx \frac{1}{\alpha\Omega}. \quad (52)$$

That is, the thermal time scale of the disk is independent of most of the disk properties and of the order $1/\alpha$ times longer than the dynamical time scale. This independence is a consequence of the α -parameterization used. If α is not a constant, but dependent on disk temper-

ature for example, the dependence of the thermal time scale on disk properties will become apparent again.

If, as seems likely from observations, α is generally < 1 , we have in thin disks the ordering of time scales:

$$t_v \gg t_t > t_d. \quad (53)$$

7 Comparison with CV observations

The number of meaningful quantitative tests between the theory of disks and observations is somewhat limited since in the absence of a theory for v , it is a bit meagre on predictive power. The most detailed information perhaps comes from modeling of CV outbursts.

Two simple tests are possible (nearly) independently of v . These are the prediction that the disk is geometrically quite thin (eq. 41) and the prediction that the surface temperature $T_s \sim r^{-3/4}$ in a steady disk. The latter can be tested in a subclass of the CV's that do not show outbursts, the nova-like systems, which are believed to be approximately steady accreters. If such a system is also eclipsing, eclipse mapping techniques can be used to derive the brightness distribution with r in the disk (Horne, 1985, 1993). If this is done in a number of colors so that bolometric corrections can be made, the results (e.g. Rutten et al. 1992) show in general a *fair* agreement with the $r^{-3/4}$ prediction. Two deviations occur: i) a few systems show significantly flatter distributions than predicted, and ii) most systems show a 'hump' near the outer edge of the disk. The latter deviation is easily explained, since we have not taken into account that the impact of the stream additionally heats the outer edge of the disk. Though not important for the total light from the disk, it is an important local contribution near the edge.

Eclipse mapping of Dwarf Novae in quiescence gives a quite different picture. Here, the inferred surface temperature profile is often nearly flat (e.g. Wood et al. 1989a, 1992). This is understandable however since in quiescence the mass flux depends strongly on r . In the inner parts of the disk it is small, near the outer edge it is close to its average value. With eq. (35), this yields a flatter $T_s(r)$. The lack of light from the inner disk is compensated during the outburst, when the accretion rate in the inner disk is higher than average (see Mineshige and Wood 1989 for a more detailed comparison). The effect is also seen in the 2-dimensional hydrodynamic simulations of accretion in a binary by Różyczka and Spruit (1993). These simulations show an outburst during which the accretion in the inner disk is enhanced, between two episodes in which mass accumulates in the outer disk.

7.1 Comparison with LMXB observations: irradiated disks

In low mass X-ray binaries a complication arises because of the much higher luminosity of the accreting object. Since a neutron star is roughly 1000 times smaller than a white dwarf, it produces 1000 times more luminosity for a given accretion rate.

Irradiation of the disk by the central source (the accreting star plus inner disk) leads to a different surface temperature than predicted by (35). The central source radiates nearly the total accretion luminosity $G\dot{M}/R$ (assuming sub-Eddington accretion, see section 2). If the disk is *concave*, it will intercept some of this luminosity. If the central source is approximated as a point source the irradiating flux on the disk surface is

$$F_{\text{irr}} = \frac{\varepsilon G\dot{M}}{2 \, 4\pi R r^2}, \quad (54)$$

where ε is the angle between the disk surface and the direction from a point on the disk surface to the central source:

$$\varepsilon = dH/dr - H/r. \quad (55)$$

The disk is concave if ε is positive. We have

$$\frac{F_{\text{irr}}}{F} = \frac{1}{3} \frac{\varepsilon}{f} \frac{r}{R},$$

where F is the flux generated internally in the disk, given by (35). On average, the angle ε is of the order of the aspect ratio $\delta = H/r$. With $f \approx 1$, and our fiducial value $\delta \approx 5 \cdot 10^{-3}$, we find that irradiation in LMXB dominates for $r \gtrsim 10^9$ cm. This is compatible with observations (for reviews see van Paradijs and McClintock 1993), which show that the optical and UV are dominated by reprocessed radiation from the innermost regions.

When irradiation by an external source is included in the thin disk model, the surface boundary condition of the radiative transfer problem, equation (38) becomes

$$\sigma_{\text{r}} T_{\text{s}}^4 = F + (1 - a) F_{\text{irr}}, \quad (56)$$

where a is the X-ray albedo of the surface, that is, $1 - a$ is the fraction of the incident flux that is absorbed in the *optically thick* layers of the disk (photons absorbed higher up only serve to heat up the corona of the disk)⁶. The surface temperature T_{s} increases in order to compensate for the additional incident heat flux. The magnitude of the incident flux is sensitive to the assumed disk shape $H(r)$, as well as on the assumed shape (plane or spherical, for example) of the central X-ray emitting region.

The disk thickness depends on temperature, and thereby also on the irradiation. It turns out, however, that this dependence on the irradiating flux is small, if the disk is optically thick and the energy transport is by radiation (Lyutyi and Sunyaev 1976). To see this, integrate (37) with the modified boundary condition (56). This yields

$$\sigma_{\text{r}} T^4 = \frac{3}{4} F \left(\tau + \frac{2}{3} \right) + (1 - a) F_{\text{irr}}. \quad (57)$$

Thus the irradiation adds an additive constant to $T^4(z)$. At the midplane, this constant has much less effect than at the surface. For the midplane temperature and the disk thickness to be affected significantly, it is necessary that

⁶ Incorrect derivations exist in the literature, in which the effect of irradiation is treated like an energy flux added to the internal viscous dissipation inside the disk rather than incident on the surface.

$$F_{\text{irr}}/F \gtrsim \tau. \quad (58)$$

The reason for this weak dependence of the midplane conditions on irradiation is the same as in radiative envelopes of stars, which are also insensitive to the surface boundary condition. The situation is different for convective disks. As in fully convective stars, the adiabatic stratification then causes the conditions at the midplane to depend much more directly on the surface temperature. The outer parts of the disks in LMXB with wide orbits are in fact convective, hence their thickness more directly affected by irradiation. This leads to the possibility of *shadowing*, with irradiated, vertically extended regions blocking irradiation of the disk outside. This plays an observable role in protostellar disks (Dullemond et al. 2001).

7.2 *Observational evidence of disk thickness*

From the paucity of sources in which eclipses of the central source by the companion are observed one deduces that the companion is barely or not at all visible as seen from the inner disk. Apparently some parts of the disk are much thicker than expected from the above arguments. This is consistent with the observation that a characteristic modulation of the optical light curve indicative of irradiation of the secondary's surface by the X-rays is not very strong in LMXB (an exception being Her X-1, which has an atypically large companion). The place of the eclipsing systems is taken by the so-called 'Accretion Disk Corona' (ADC) systems, where shallow eclipses of a rather extended X-ray source are seen instead of the expected sharp eclipses of the inner disk (for reviews of the observations, see Lewin et al. 1995). The conclusion is that there is an extended X-ray scattering 'corona' above the disk. It scatters a few per cent of the X-ray luminosity.

What causes this corona and the large inferred thickness of the disk? The thickness expected from disk theory is a rather stable small number. To 'suspend' matter at the inferred height of the disk forces are needed that are much larger than the pressure forces available in an optically thick disk. A thermally driven wind, produced by X-ray heating of the disk surface, has been invoked (Begelman et al. 1983, Schandl and Meyer 1994, 1997). For other explanations, see van Paradijs and McClintock (1995). Perhaps a magnetically driven wind from the disk (e.g. Bisnovatyi-Kogan & Ruzmaikin 1976, Blandford & Payne 1982), such as inferred for protostellar objects (cf. Lee et al. 2000) can explain both the shielding of the companion and the scattering. Such a model would resemble magnetically driven wind models for the broad-line region in AGN (e.g. Emmering et al., 1992, Königl and Kartje 1994). A promising possibility is that the reprocessing region consists of matter 'kicked up' at the disk edge by the impact of the mass transferring stream (Meyer-Hofmeister et al. 1997, Armitage and Livio 1998, Spruit et al. 1998). This produces qualitatively the right dependence of X-ray absorption on orbital phase in ADC sources, and the light curves of the so-called supersoft sources.

7.3 Transients

Soft X-ray transients (also called X-ray Novae) are believed to be binaries similar to the other LMXB, but somehow the accretion is episodic, with very large outbursts recurring on time scales of decades (sometimes years). Most of these transients turn out to be black hole candidates (see Lewin et al. 1995 for a review). As with the Dwarf Novae, the time dependence of the accretion can in principle be exploited in transients to derive information on the disk viscosity, assuming that the outburst is caused by an instability in the disk. The closest relatives of soft transients among the White Dwarf plus main sequence star systems are probably the WZ Sge stars (van Paradijs and Verbunt 1984, Kuulkers et al. 1996), which show (in the optical) similar outbursts with similar recurrence times (cf. Warner 1987, O'Donoghue et al. 1991). Like the soft transients, they have low mass ratios ($q < 0.1$). For a given angular momentum loss, systems with low mass ratios have low mass transfer rates, so the speculation is that the peculiar behavior of these systems is somehow connected in both cases with a low mean accretion rate.

7.3.1 Transients in quiescence

X-ray transients in quiescence (i.e. after an outburst) usually show a very low X-ray luminosity. The mass transfer rate from the secondary in quiescence can be inferred from the optical emission. This shows the characteristic 'hot spot', known from other systems to be the location where the mass transferring stream impacts on the edge of an accretion disk (e.g. van Paradijs and McClintock 1995). These observations thus show that a disk is present in quiescence, while the mass transfer rate can be measured from the brightness of the hot spot. If this disk were to extend to the neutron star with constant mass flux, the predicted X-ray luminosity would be much higher than observed. This has traditionally been interpreted as a consequence of the fact that in transient systems, the accretion is not steady. Mass is stored in the outer parts and released by a disk instability (e.g. King 1995, Meyer-Hofmeister and Meyer 1999) producing the X-ray outburst. During quiescence, the accretion rate onto the compact object is much smaller than the mass transfer from the secondary to the disk.

7.4 Disk Instability

The most developed model for outbursts is the disk instability model of Osaki (1974), Hōshi (1979), Smak (1971, 1984), Meyer and Meyer-Hofmeister (1981), see also King (1995), Osaki (1993). In this model the instability that gives rise to cyclic accretion is due to a temperature dependence of the viscous stress. In any local process that causes an effective viscosity, the resulting α -parameter will be a function of the main dimensionless parameter of the disk, the aspect ratio H/r . If this is a sufficiently rapidly increasing function, such that α is large in hot disks and low in cool disks, an instability results by the following mechanism. Suppose we start the disk in a stationary state at the mean accretion rate. If this state is perturbed by a small temperature increase, α goes up, and by the increased viscous stress the mass flux \dot{M}

increases. By (35) this increases the disk temperature further, resulting in a runaway to a hot state. Since \dot{M} is larger now than the average, the disk empties partly, reducing the surface density and the central temperature (eq. 40). A cooling front then transforms the disk to a cool state with an accretion rate below the mean. The disk in this model switches back and forth between hot and cool states. By adjusting the value of α in the hot and cool states, or by adjusting the functional dependence of α on H/r , outbursts are obtained that agree reasonably with the observations of soft transients (Lin and Taam 1984, Mineshige and Wheeler, 1989). A rather strong increase of α with H/r is needed to get the observed long recurrence times.

Another possible mechanism for instability has been found in 2-D numerical simulations of accretion disks (Blaes and Hawley 1988, Różyczka and Spruit 1993). The outer edge of a disk is found, in these simulations, to become dynamically unstable to an oscillation which grows into a strong eccentric perturbation (a crescent shaped density enhancement which rotates at the local orbital period). Shock waves generated by this perturbation spread mass over most of the Roche lobe; at the same time the accretion rate onto the central object is strongly enhanced. This process is different from the Smak-Osaki-Hōshi mechanism, since it requires 2 dimensions, and does not depend on the viscosity (instead, the internal dynamics in this instability *generates* the effective viscosity that causes a burst of accretion).

7.5 Other Instabilities

Instability to heating/cooling of the disk can be due to several effects. The cooling rate of the disk, if it depends on temperature in an appropriate way, can cause a thermal instability like that in the interstellar medium. Other instabilities may result from the dependence of viscosity on conditions in the disk. For a general treatment see Piran (1978), for a shorter discussion see Treves et al. (1988).

8 Sources of Viscosity

The high Reynolds number of the flow in accretion disks (of the order 10^{14} in the outer parts of a CV disk) would, to most fluid dynamicists, seem an amply sufficient condition for the occurrence of hydrodynamic turbulence (see also the discussion in section 4.7). A theoretical argument against such turbulence often used in astrophysics (Kippenhahn and Thomas 1981, Pringle 1981) is that in cool disks the gas moves almost on Kepler orbits, which are quite stable (except for the orbits that get close to the companion or near a black hole). This stability is related to the known stabilizing effect that rotation has on hydrodynamical turbulence (Bradshaw 1969, Lesur & Longaretti 2005). A (not very strong) observational argument is that hydrodynamical turbulence as described above would produce an α that does not depend on the nature of the disk, so that all objects should have the same value, which is not what observations show. From the modeling of CV outbursts one knows, for example, that α probably increases with temperature (more accurately, with H/r , see previous section).

Also, there are indications from the inferred life times and sizes of protostellar disks (Strom et al. 1993) that α may be rather small there, $\sim 10^{-3}$, whereas in outbursts of CV's one infers values of the order 0.1 – 1.

Among the processes that have been proposed repeatedly as sources of viscosity is convection due to a vertical entropy gradient (e.g. Kley et al. 1993), which may have some limited effect in convective parts of disks. Rotation rate varies somewhat with height in a disk, due to the radial temperature gradient ('baroclinicity'). Modest amounts of turbulence have been reported from instability of this form of differential rotation (Klahr & Bodenheimer 2003, Lesur and Papaloizou 2010).

Another class are *waves* of various kinds. Their effect can be global, that is, not reducible to a local viscous term because by traveling across the disk they can communicate torques over large distances. For example, waves set up at the outer edge of the disk by tidal forces can travel inward and by dissipating there can effectively transport angular momentum *outward* (e.g. Narayan et al. 1987, Spruit et al. 1987). A nonlinear version of this idea are selfsimilar spiral shocks, observed in numerical simulations (Sawada et al. 1987) and studied analytically (Spruit 1987). Such shocks can produce accretion at an effective α of 0.01 in hot disks, but are probably not very effective in disks as cool as those in CV's and XRB.

A second non-local mechanism is provided by a magnetically accelerated *wind* originating from the disk surface (Blandford 1976, Bisnovaty-Kogan and Ruzmaikin 1976, Lovelace 1976, for an introduction see Spruit 1996). In principle, such winds can take care of *all* the angular momentum loss needed to make accretion possible in the absence of a viscosity (Blandford 1976, Königl 1989). The attraction of this idea is that magnetic winds are a strong contender for explaining the strong outflows and jets seen in some protostellar objects and AGN. It is not yet clear however if, even in these objects, the wind is actually the main source of angular momentum loss.

In sufficiently cool or massive disks, selfgravitating instabilities of the disk matter can produce internal friction. Paczyński (1978) proposed that the resulting heating would limit the instability and keep the disk in a well defined moderately unstable state. The angular momentum transport in such a disk has been studied numerically (e.g. Gammie 1997, Ostriker et al. 1999). Disks in CVs and XRB are too hot for selfgravity to play a role, but it can be important in protostellar disks (cf. Rafikov 2009).

8.1 magnetic viscosity

Magnetic forces can be very effective at transporting angular momentum. If it can be shown that the shear flow in the disk produces some kind of small scale fast dynamo process, that is, some form of magnetic turbulence, an effective $\alpha \sim O(1)$ would be expected (Shakura and Sunyaev 1973). Numerical simulations of initially weak magnetic fields in accretion disks show that this does indeed happen in sufficiently ionized disks (Hawley et al. 1995, Brandenburg et al. 1995, Balbus 2003). These show a small scale magnetic field with azimuthal component dominating (due to stretching by differential rotation). The angular momentum transport is due to magnetic stresses, the fluid motions induced by the magnetic forces contribute only little to the angular momentum transport. In a perfectly conducting plasma this

turbulence can develop from an arbitrarily small initial field through magnetic shear instability (also called magnetorotational instability, Velikhov 1959, Chandrasekhar 1961, Balbus and Hawley 1991). The significance of this instability is that it shows that at large conductivity accretion disks must be magnetic.

The actual form of the highly time dependent small scale magnetic field which develops can only be found from numerical simulations. The simplest case thought to be representative of the process considers a vertically unstratified disk (component of gravity perpendicular to the disk ignored), of which only a radial extent of a few times H is included (cf. the causality argument above). Different simulations have yielded somewhat different values for the effective viscosity, contrary to the expectation that at least in this simplest form the process should yield a unique value.

The nature of these differences has been appreciated only recently. Fromang et al. (2007a) show that the results do not converge with increasing numerical resolution (the effective α found appears to decrease indefinitely). The result also depends on the magnetic Prandtl number $P_m = \nu/\eta_m$, the ratio of viscosity to magnetic diffusivity η_m . No turbulence is found for $P_m < 1$ Fromang et al. (2007b). The significance of these findings is not quite obvious yet, but they clearly contradict the commonly assumed ‘cascade’ picture of MHD turbulence (taken over from what is assumed in hydrodynamic turbulence, where the large scale behavior of turbulence appears to converge with numerical resolution).

Perhaps the behavior found in this case is related to the highly symmetric nature of the idealized problem. This is suggested by the finding (Davis et al. 2010, Shi et al. 2010) that effective viscosity appears to converge again with increasing numerical resolution when vertical stratification is included. By inference, the process defining the state of magnetic turbulence is different in this case from that in the unstratified case. It can plausibly be attributed to magnetic buoyancy instabilities (Shi et al. 2010). This would make the process somewhat analogous to the mechanism operating the solar cycle (Spruit 2010). Magnetic turbulence also behaves different if the net vertical magnetic flux crossing the simulated box does not vanish. (This flux is a conserved quantity set by the initial conditions). Magnetic turbulence then develops more easily (at lower numerical resolution), and appears to converge as the numerical resolution is increased.

The consequences of these new findings for angular momentum transport in disks are still to be settled (c.f. the insightful discussion in Lesur and Ogilvie 2008).

8.2 *viscosity in radiatively supported disks*

A disk in which the radiation pressure P_r dominates must be optically thick (otherwise the radiation would escape). The radiation pressure then adds to the total pressure. The pressure is larger than it would be, for a given temperature, if only the gas pressure were effective. If the viscosity is then parametrized by (19), it turns out (Lightman and Eardley, 1974) that the disk is locally unstable. An increase in temperature increases the radiation pressure, which increases the viscous dissipation and the temperature, leading to a runaway. This has raised the question whether the radiation pressure should be included in the sound speed that enters expression (19). If it is left out, a lower viscosity results, and there is no thermal-viscous run-

away. Without knowledge of the process causing the effective viscous stress, this question can not be answered. Sakimoto and Coroniti (1989) have shown, however, that if the stress is due to some form of magnetic turbulence, it most likely scales with the gas pressure alone, rather than the total pressure. Now that it seems likely, from the numerical simulations, that the stress is indeed magnetic, there is reason to believe that in the radiation pressure-dominated case the effective viscosity will scale as $\nu \sim \alpha P_g / (\rho \Omega)$, making such disks thermally stable, as indicated by the results of Hirose et al. (2009).

9 Beyond thin disks

Ultimately, much of the progress in developing useful models of accretion disks will depend on detailed numerical simulations in 2 or 3 dimensions. In the disks one is interested in, there is usually a large range in length scales (in LMXB disks, from less than the 10 km neutron star radius to the more than 10^5 km orbital scale). Correspondingly, there is a large range in time scales that have to be followed. This not technically possible at present and in the foreseeable future. In numerical simulations one is therefore limited to studying in an approximate way aspects that are either local or of limited dynamic range in r, t (for examples, see Hawley 1991, Armitage 1998, De Villiers et al. 2003, Hirose et al. 2004). For this reason, approaches have been used that relax the strict thin disk framework somewhat without resorting to full simulations. Some of the physics of thick disks can be included in a fairly consistent way in the ‘slim disk’ approximation (Abramowicz et al., 1988). The so-called Advection Dominated Accretion Flows (ADAFs) are related to this approach (for a review see Yi 1998). They are discussed in sections 11, 12, 13 below).

9.1 Boundary layers

In order to accrete onto a star rotating at the rate Ω_* , the disk matter must dissipate an amount of energy given by

$$\frac{GM\dot{M}}{2R} [1 - \Omega_*/\Omega_k(R)]^2. \quad (59)$$

The factor in brackets measures the kinetic energy of the matter at the inner edge of the disk ($r = R$), in the frame of the stellar surface. Due to this dissipation the disk inflates into a ‘belt’ at the equator of the star, of thickness D and radial extent of the same order. Equating the radiation emitted from the surface of this belt to (59) one gets for the surface temperature T_{sb} of the belt, assuming optically thick conditions and a slowly rotating star ($\Omega_*/\Omega_k \ll 1$):

$$\frac{GM\dot{M}}{8\pi R^2 D} = \sigma_{\text{r}} T_{\text{sb}}^4 \quad (60)$$

To find the temperature inside the belt and its thickness, use eq. (39). The value of the surface temperature is higher, by a factor of the order $(R/D)^{1/4}$, than the simplest thin disk estimate

(35, ignoring the factor f). In practice, this works out to a factor of a few. The surface of the belt is therefore not very hot. The situation is quite different if the boundary layer is not optically thick (Pringle and Savonije 1979). It then heats up to much higher temperatures.

Analytical methods to obtain the boundary layer structure have been used by Regev and Hougerat (1988), numerical solutions of the slim disk type by Narayan and Popham (1993), Popham (1997), 2-D numerical simulations by Kley (1991). These considerations are primarily relevant for CV disks; in accreting neutron stars, the dominant effects of radiation pressure have to be included. More analytic progress on the structure of the boundary layer between a disk and a neutron star and the way in which it spreads over the surface of the star has been reported by Inogamov and Sunyaev (1999).

10 Radiative efficiency of accretion disks

In a thin accretion disk, the time available for the accreting gas to radiate away the energy released by the viscous stress is the accretion time,

$$t_{\text{acc}} \approx \frac{1}{\alpha \Omega_K} \left(\frac{r}{H} \right)^2, \quad (61)$$

where α is the dimensionless viscosity parameter, Ω_K the local Keplerian rotation rate, r the distance from the central mass, and H the disk thickness (see Frank et al. 2002 or section 6). For a thin disk, $H/r \ll 1$, this time is much longer than the thermal time scale $t_t \approx 1/(\alpha \Omega)$ (section 6). There is then enough time for a local balance to hold between viscous dissipation and radiative cooling. For the accretion rates implied in observed systems the disk is then rather cool, which then justifies the starting assumption $H/r \ll 1$.

This argument is somewhat circular, of course, since the accretion time is long enough for effective cooling only if the disk is assumed to be thin to begin with. Other forms of accretion disks may exist, even at the same accretion rates, in which the cooling is ineffective compared with that of standard (geometrically thin, optically thick) disks. In the following sections, we consider such forms of accretion and the conditions under which are to be expected.

Since radiatively inefficient disks tend to be thick, $H/r \sim O(1)$, they are sometimes called ‘quasi-spherical’. However, this does *not* mean that a spherically symmetric accretion model would be a reasonable approximation. The crucial difference is that the flow has angular momentum. The inward flow speed is governed by the rate at which angular momentum can be transferred outwards, rather than by gravity and pressure gradient as in the Bondi accretion problem mentioned above. With $H/r \sim O(1)$, the accretion time scale, $t_{\text{acc}} \sim 1/(\alpha \Omega)$ is still longer than the accretion time scale in the spherical case, $1/\Omega$, (unless the viscosity parameter α is as large as $O(1)$). The dominant velocity component is azimuthal rather than radial, and the density and optical depth are much larger than in the spherical case.

It turns out that there are two kinds of radiatively inefficient disks, the optically thin and optically thick varieties. A second distinction occurs because accretion flows are different for central objects with a solid surface (neutron stars, white dwarfs, main sequence stars, planets), and those without (i.e. black holes). Start with optically thick flows.

11 Radiation supported radiatively inefficient accretion

If the energy loss by radiation is small, the gravitational energy release $W_{\text{grav}} \approx GM/(2r)$ is converted into enthalpy of the gas and radiation field⁷

$$\frac{1}{2} \frac{GM}{r} = \frac{1}{\rho} \left[\frac{\gamma}{\gamma-1} P_g + 4P_r \right], \quad (62)$$

where an ideal gas of constant ratio of specific heats γ has been assumed, and $P_r = \frac{1}{3}aT^4$ is the radiation pressure. In terms of the virial temperature $T_{\text{vir}} = GM/(\mathcal{R}r)$, and assuming $\gamma = 5/3$, appropriate for a fully ionized gas (see section 2.1), this can be written as

$$\frac{T}{T_{\text{vir}}} = \left[5 + 8 \frac{P_r}{P_g} \right]^{-1}. \quad (63)$$

Thus, for radiation pressure dominated accretion, $P_r \gg P_g$, the temperature is much less than the virial temperature: much of the accretion energy goes into photon production instead of heating. By hydrostatic equilibrium the disk thickness is given by (cf section 4.2)

$$H \approx [(P_g + P_r)/\rho]^{1/2}/\Omega, \quad (64)$$

With (63) this yields

$$H/r \sim O(1). \quad (65)$$

In the limit $P_r \gg P_g$, the flow is therefore geometrically thick. Radiation pressure then supplies a non-negligible fraction of the support of the gas in the radial direction against gravity (the remainder being provided by rotation).

For $P_r \gg P_g$, (62) yields

$$\frac{GM}{2r} = \frac{4}{3} \frac{aT^4}{\rho}. \quad (66)$$

The radiative energy flux, in the diffusion approximation, is (eq. 37)

$$F = \frac{4}{3} \frac{d}{d\tau} \sigma_r T^4 \approx \frac{4}{3} \frac{\sigma_r T^4}{\tau}. \quad (67)$$

Hence

$$F = \frac{1}{8} \frac{GM}{rH} \frac{c}{\kappa} = F_E \frac{r}{8H}, \quad (68)$$

where $F_E = L_E/(4\pi r^2)$ is the local Eddington flux. Since $H/r \approx 1$, a radiatively inefficient, radiation pressure dominated accretion flow has a luminosity of the order of the Eddington luminosity.

The temperature depends on the accretion rate and the viscosity ν assumed. The accretion rate is of the order $\dot{M} \sim 3\pi\nu\Sigma$ (cf. eq. (29)), where $\Sigma = \int \rho dz$ is the surface mass density. In units of the Eddington rate \dot{M}_E , eq. (8), we get

⁷ This assumes that a fraction ~ 0.5 of the gravitational potential energy stays in the flow as orbital kinetic energy. This is only an approximation, see also section 12.

$$\dot{m} \equiv \dot{M}/\dot{M}_E \approx v\rho\kappa/c, \quad (69)$$

where $H/r \approx 1$ has been used⁸. Assume that the viscosity scales with the gas pressure:

$$v = \alpha \frac{P_g}{\rho\Omega_K}, \quad (70)$$

instead of the total pressure $P_r + P_g$. This is the form that is likely to hold if the angular momentum transport is due to a small-scale magnetic field (Sakimoto and Coroniti, 1989, Turner 2004). Then with (66), (69) we have (up to a numerical factor of $\mathcal{O}(1)$)

$$T^5 \approx \frac{(GM)^{3/2}}{r^{5/2}} \frac{\dot{m}c}{\alpha\kappa a\mathcal{R}}, \quad (71)$$

or

$$T \approx 10^8 r_6^{-1/5} (r/r_g)^{3/10} \dot{m}^{1/5}, \quad (72)$$

where $r = 10^6 r_6$ and $r_g = 2GM/c^2$ is the gravitational radius of the accreting object, and the electron scattering opacity of $0.3 \text{ cm}^2/\text{g}$ has been assumed. The temperatures expected in radiation supported advection dominated flows are therefore quite low compared with the virial temperature [If the viscosity is assumed to scale with the total pressure instead of P_g , the temperature is even lower]. The effect of electron-positron pairs can be neglected (Schultz and Price, 1985), since they are present only at temperatures approaching the electron rest mass energy, $T \gtrsim 10^9 \text{ K}$.

In order for the flow to be radiation pressure and advection dominated, the optical depth has to be sufficiently large so the radiation does not leak out. The energy density in the flow, vertically integrated is of the order

$$E \approx aT^4 H, \quad (73)$$

and the energy loss rate per cm^2 of disk surface is given by (68). The cooling time is therefore,

$$t_c = E/F = 3\tau H/c. \quad (74)$$

This is to be compared with the accretion time, which can be written in terms of the mass in the disk at radius r , of the order $2\pi r^2 \Sigma$, and the accretion time:

$$t_{\text{acc}} \approx 2\pi r^2 \Sigma / \dot{M}. \quad (75)$$

This yields

$$t_c/t_{\text{acc}} \approx \frac{\kappa}{\pi r c} \dot{M} = \frac{4}{\eta} \frac{R}{r}, \quad (76)$$

(where a factor $3/2H/r \sim O(1)$ has been neglected). Since $r > R$, this shows that accretion has to be around the Eddington rate or larger in order to be both radiation- and advection-dominated.

⁸ The definition of \dot{M}_E differs by factors of order unity between different authors. It depends on the assumed efficiency η of conversion of gravitational energy GM/R into radiation. For accretion onto black holes a more realistic value is of order $\eta = 0.1$, for accretion onto neutron stars $\eta \approx 0.4$, depending on the radius of the star.

This condition can also be expressed in terms of the so-called *trapping radius* r_t (e.g. Rees 1978). Equating t_{acc} and t_c yields

$$r_t/R \approx 4\dot{m}. \quad (77)$$

Inside r_t , the flow is advection dominated: the radiation field produced by viscous dissipation stays trapped inside the flow, instead of being radiated from the disk as happens in a standard thin disk. Outside the trapping radius, the radiation field cannot be sufficiently strong to maintain a disk with $H/r \sim 1$, it must be a thin form of disk instead. Such a thin disk can still be radiation-supported (i.e. $P_r \gg P_g$), but it can not be advection dominated.

Flows of this kind are called ‘radiation supported accretion tori’ (or radiation tori, for short) by Rees et al. 1982. They must accrete at a rate above the Eddington value to exist. The converse is not quite true: a flow accreting above Eddington is an advection dominated flow, but it need not necessarily be radiation dominated. Advection dominated optically thick accretion flows exist in which radiation does not play a major role (see section 12.1).

That an accretion flow above \dot{M}_E is advection dominated, not a thin disk, also follows from the fact that in a thin disk the energy dissipated must be radiated away locally. Since the local radiative flux can not exceed the Eddington energy flux F_E , the mass accretion rate in a thin disk can not significantly exceed the Eddington value (8).

The gravitational energy, dissipated by viscous stress in differential rotation and advected with the flow, ends up on the central object. If this is a black hole, the photons, particles and their thermal energy are conveniently swallowed at the horizon, and do not react back on the flow. Radiation tori are therefore mostly relevant for accretion onto black holes. They are convectively unstable (Bisnovatyi-Kogan and Blinnikov 1977): the way in which energy is dissipated, in the standard α -prescription, is such that the entropy (entropy of radiation, $\sim T^3/\rho$) decreases with height in the disk. Numerical simulations (see section 14) show the effects of this convection.

11.1 Super-Eddington accretion onto black holes

As the accretion rate onto a black hole is increased above \dot{M}_E , the trapping radius moves out. The total luminosity increases only slowly, and remains of the order of the Eddington luminosity. Such supercritical accretion has been considered by Begelman and Meier (1982, see also Wang and Zhou 1999); they show that the flow has a radially self-similar structure.

Abramowicz et al. (1988, 1989) studied accretion onto black holes at rates near \dot{M}_E . They used a vertically-integrated approximation for the disk, but included the advection terms. The resulting models were called ‘slim disks’. They show how with increasing accretion rate, a standard thin Shakura-Sunyaev disk turns into a radiation-supported advection flow. The nature of the transition depends on the viscosity prescription used, and can show a non-monotonic dependence of \dot{M} on surface density Σ (Honma et al. 1991). This suggests the possibility of instability and cyclic behavior of the inner disk near a black hole, at accretion rates near and above \dot{M}_E (for an application to GRS 1915+105 see Nayakshin et al., 1999).

11.2 Super-Eddington accretion onto neutron stars

In the case of accretion onto a neutron star, the energy trapped in the flow, plus the remaining orbital energy, settles onto its surface. If the accretion rate is below \dot{M}_E , the energy can be radiated away by the surface, and steady accretion is possible. A secondary star providing the mass may, under some circumstances, transfer more than \dot{M}_E , since it does not know about the neutron star's Eddington value. The outcome of this case is still somewhat uncertain; it is generally believed on intuitive grounds that the 'surplus' (the amount above \dot{M}_E) somehow gets expelled from the system.

One possibility is that, as the transfer rate is increased, the accreting hot gas forms an extended atmosphere around the neutron star like the envelope of a giant. If it is large enough, the outer parts of this envelope are partially ionized. The opacity in these layers, due to atomic transitions of the CNO and heavier elements, is then much higher than the electron scattering opacity. The Eddington luminosity based on the local value of the opacity is then smaller than it is near the neutron star surface. Once an extended atmosphere forms, the accretion luminosity is thus large enough to drive a wind from the envelope (see Kato 1997, where the importance of this effect is demonstrated in the context of Novae).

This scenario is somewhat dubious however, since it assumes that the mass transferred from the secondary continues to reach the neutron star and generate a high luminosity there. This is not at all obvious, since the mass transferring stream may instead dissipate inside the growing envelope of the neutron star. The result of this could be a giant (more precisely, a Thorne-Zytkow star), with a steadily increasing envelope mass. Such an envelope is likely to be large enough to engulf the entire binary system, which then develops into a common-envelope (CE) system. The envelope mass is then expected to be ejected by CE hydrodynamics (for reviews see Taam 1994, Taam and Sandquist 2000).

A more speculative proposal, suggested by the properties of SS 433, is that the 'surplus mass' is ejected in the form of jets. The binary parameters of Cyg X-2 are observational evidence for mass ejection in super-Eddington mass transfer phases (King and Ritter 1999, Rappaport and Podsiadlowski 2000, King and Begelman 1999).

12 ADAF Hydrodynamics

The hydrodynamics of radiatively inefficient flows (or 'advection dominated accretion flows') can be studied by starting, at a very simple level, with a generalization of the thin disk equations. Making the assumption that quantities integrated over the height z of the disk give a fair representation (though this is justifiable only for thin disks), and assuming axisymmetry, the problem reduces to a one-dimensional time-dependent one. Further simplifying this by restriction to a steady flow yields the equations

$$2\pi r \Sigma v_r = \dot{M} = \text{cst}, \quad (78)$$

$$r \Sigma v_r \partial_r (\Omega r^2) = \partial_r (v \Sigma r^3 \partial_r \Omega), \quad (79)$$

$$v_r \partial_r v_r - (\Omega^2 - \Omega_K^2) r = -\frac{1}{\rho} \partial_r P, \quad (80)$$

$$\Sigma v_r T \partial_r S = q^+ - q^-, \quad (81)$$

where S is the specific entropy of the gas, Ω the local rotation rate, now different from the Keplerian rate Ω_K , and

$$q^+ = \int Q_v dz \quad q^- = \int \text{div} F_r dz \quad (82)$$

are the height-integrated viscous dissipation rate and radiative loss rate, respectively. In the case of thin disks, equations (78) and (79) are unchanged, but (80) simplifies to $\Omega^2 = \Omega_K^2$, i.e. the rotation is Keplerian, while (81) simplifies to $q^+ = q^-$, expressing local balance between viscous dissipation and cooling. The left hand side of (81) describes the radial advection of heat, and is perhaps the most important deviation from the thin disk equations at this level of approximation (hence the name advection dominated flows). The characteristic properties are seen most clearly when radiative loss is neglected altogether, $q^- = 0$. The equations are supplemented with expressions for v and q^+ :

$$v = \alpha c_s^2 / \Omega_K; \quad q^+ = (r \partial_r \Omega)^2 v \Sigma. \quad (83)$$

If α is taken constant, $q^- = 0$, and an ideal gas is assumed with constant ratio of specific heats, so that the entropy is given by

$$S = c_v \ln(p/\rho^\gamma), \quad (84)$$

then equations (78)-(81) have no explicit length scale in them. This means that a special so-called self-similar solution exists, in which all quantities are powers of r . Such self-similar solutions have apparently been described first by Gilham (1981), but re-invented several times (Spruit et al. 1987; Narayan and Yi, 1994). The dependences on r are

$$\Omega \sim r^{-3/2}; \quad \rho \sim r^{-3/2}, \quad (85)$$

$$H \sim r; \quad T \sim r^{-1}. \quad (86)$$

In the limit $\alpha \ll 1$, one finds

$$v_r = -\alpha \Omega_K r \left(9 \frac{\gamma-1}{5-\gamma} \right), \quad (87)$$

$$\Omega = \Omega_K \left(2 \frac{5-3\gamma}{5-\gamma} \right)^{1/2}, \quad (88)$$

$$c_s^2 = \Omega_K^2 r^2 \frac{\gamma-1}{5-\gamma}, \quad (89)$$

$$\frac{H}{r} = \left(\frac{\gamma-1}{5-\gamma} \right)^{1/2}. \quad (90)$$

The precise form of these expressions depends somewhat on the way in which vertical integrations such as in (82) are done (which are only approximate).

The self-similar solution can be compared with numerical solutions of eqs. (78)–(81) with appropriate conditions applied at inner (r_i) and outer (r_o) boundaries (Nakamura et al. 1996, Narayan et al. 1997). The results show that the self-similar solution is valid in an intermediate regime $r_i \ll r \ll r_o$. That is, the solutions of (78)–(81) approach the self-similar solution far from the boundaries, as is characteristic of self-similar solutions.

The solution exists only if $1 < \gamma \leq 5/3$, a condition satisfied by all ideal gases. As $\gamma \downarrow 1$, the disk temperature and thickness vanish. This is understandable, since a γ close to 1 means that the particles making up the gas have a large number of internal degrees of freedom. In thermal equilibrium the accretion energy is shared between all degrees of freedom, so that for a low γ less is available for the kinetic energy (temperature) of the particles.

Second, the *rotation rate vanishes* for $\gamma \rightarrow 5/3$. As in the case of spherical accretion no accreting solutions exist for $\gamma > 5/3$ (cf. section 2). Since a fully ionized gas has $\gamma = 5/3$, it is a relevant value for the hot, ion supported accretion flows discussed below. Apparently, steady advection dominated accretion can not have angular momentum in this case. To see how comes about consider the entropy of the flow. For accretion to take place in a rotating flow, there has to be friction and increase of entropy. Accretion is then necessarily accompanied by an inward increase of entropy. In a radially self similar flow, the scalings (85), (86) yield $P \sim r^{-5/2}$, so entropy scales as $S \sim \ln P/\rho^\gamma \sim (5 - 3\gamma) \ln r$. This increases with decreasing distance r only for $\gamma < 5/3$, and an accretion flow with $\gamma = 5/3$ cannot be both rotating and adiabatic. (With energy losses by radiation the constraint on γ disappears again).

The question then arises how an adiabatic flow with $\gamma = 5/3$ will behave if one starts it as a rotating torus around a black hole. In the literature, this problem has been circumvented by arguing that real flows would have magnetic fields in them, which would change the effective compressibility of the gas. Even if a magnetic field of sufficient strength is present, however, (energy density comparable to the gas pressure) the effective γ is not automatically lowered. If the field is compressed mainly perpendicular to the field lines, for example, the effective γ is closer to 2. Also, this does not solve the conceptual problem what would happen to a rotating accretion flow consisting of a more weakly magnetized ionized gas.

12.0.1 The case of the vanishing rotation rate

This conceptual problem has been solved by Ogilvie (1999), who showed how a gas cloud initially rotating around a point mass settles to the slowly rotating self-similar solutions of the steady problem discussed above. He constructed similarity solutions to the time dependent version of eqs (78)–(81), in which distance and time occur in the combination $r/t^{2/3}$. This solution describes the asymptotic behavior (in time) of a viscously spreading disk, analogous to the viscous spreading of thin disks (see section 4.3). As in the thin disk case, all the mass accretes asymptotically onto the central mass, while all the angular momentum travels to infinity together with a vanishing amount of mass. For all $\gamma < 5/3$, the rotation rate at a fixed r tends to a finite value as $t \rightarrow \infty$, but for $\gamma = 5/3$ it tends to zero. The size of the slowly-rotating region expands as $r \sim t^{2/3}$. The typical slow rotation of ADAFs at γ near $5/3$ is thus a real physical property. In such a flow the angular momentum gets expelled from the

inner regions almost completely, and the accretion flow becomes purely radial, as in Bondi accretion.

12.1 Other optically thick accretion flows

The radiation-dominated flows discussed in section 11 are not the only possible optically thick advection dominated flows. From the discussion of the hydrodynamics, it is clear that disk-like (i.e. rotating) accretion is possible whenever the ratio of specific heats is less than $5/3$. A radiation supported flow satisfies this requirement since radiation pressure scales with volume like a gas with $\gamma = 4/3$, but it can also happen in the absence of radiation if energy is taken up in the gas by internal degrees of freedom of the particles. Examples are the rotational and vibrational degrees of freedom in molecules, and the energy associated with dissociation and ionization. If the accreting object has a gravitational potential not too far from the $2.3 + 13.6$ eV per proton for dissociation plus ionization, a gas initially consisting of molecular hydrogen can stay bound at arbitrary accretion rates. This translates into a limit $M/M_{\odot} R_{\odot}/R < 0.01$. This is satisfied approximately by the giant planets, which are believed to have gone through a phase of rapid adiabatic gas accretion (e.g. Podolak et al. 1993).

A more remotely related example is the core-collapse supernova. The accretion energy of the core mass falling onto the growing proto-neutron star at its center is lost mostly to internal degrees of freedom represented by photodisintegration of the nuclei. If the pre-collapse core rotates sufficiently rapidly, the collapse will form an accretion torus (inside the supernova envelope), with properties similar to advection dominated accretion flows (but at extreme densities and accretion rates, by X-ray binary standards). Such objects have been invoked as sources of Gamma-ray bursts (Woosley 1993, Paczyński 1998, Popham et al. 1999).

A final possibility for optically thick accretion is through *neutrino losses*. If the temperature and density near an accreting neutron star become large enough, additional cooling takes place through neutrinos (as in the cores of giants). This is relevant for the physics of Thorne-Zytkow stars (neutron stars or black holes in massive supergiant envelopes, cf. Bisnovatyi-Kogan and Lamzin 1984, Cannon et al. 1992), and perhaps for the spiral-in of neutron stars into giants (Chevalier 1993, see however Taam & Sandquist 2000).

13 Optically thin radiatively inefficient flows (ISAFs)

The optically thin case has received most attention, because of the promise it holds for explaining the (radio to X-ray) spectra of X-ray binaries and the central black holes in galaxies, including our own. For a review see Yi (1999). This kind of flow occurs if the gas is optically thin, and radiation processes are sufficiently weak. The gas then heats up to near the virial temperature. Near the last stable orbit of a black hole, this is of the order 100 MeV, or 10^{12} K. At such temperatures, a gas in thermal equilibrium would radiate at a fantastic rate, even if it were optically thin, because the interaction between electrons and photons becomes very strong already near the electron rest mass of 0.5 MeV. In a remarkable early paper, Shapiro,

Lightman and Eardley (1976) noted that this, however, is not what will happen in an optically thin plasma accreting on a hole. They showed that instead thermal equilibrium between ions and electrons breaks down and a *two-temperature plasma* forms. We call such a flow an ion supported accretion flow (ISAF), following the nomenclature suggested by Rees et al. (1982). The argument is as follows.

Suppose that the energy released by viscous dissipation is distributed equally among the carriers of mass, i.e. mostly to the ions and $\sim 1/2000$ to the electrons. Most of the energy then resides in the ions, which radiate very inefficiently (their high mass prevents the rapid accelerations that are needed to produce electromagnetic radiation). Their energy is transferred to the electrons by Coulomb interactions. These interactions are slow, however, under the conditions mentioned. They are slow because of the low density (on account of the assumed low optical thickness), and because they decrease with increasing temperature. The electric forces that transfer energy from an ion to an electron act only as long as the ion is within the electron's Debye sphere (e.g. Spitzer, 1965). The interaction time between proton and electron, and thus the momentum transferred, therefore decrease as $1/\nu_p \sim T_p^{-1/2}$ where T_p is the proton temperature.

In this way, an optically thin plasma near a compact object can be in a two-temperature state, with the ions being near the virial temperature and the electrons, which are doing the radiating, at a much lower temperature around 50–200 keV. The energy transfer from the gravitational field to the ions is fast (by some form of viscous or magnetic dissipation, say), from the ions to the electrons slow, and finally the energy losses of the electrons fast (by synchrotron radiation in a magnetic field or by inverse Compton scattering off soft photons). Such a flow would be radiatively inefficient since the receivers of the accretion energy, the ions, get swallowed by the hole before having a chance to transfer their energy to the electrons. Most of the accretion energy thus gets lost into the hole, and the radiative efficiency is much less than for a cool disk. The first disk models which take into account this physics of advection and a two-temperature plasma were developed by Ichimaru (1977).

It is clear from this description that both the physics of such flows and the radiation spectrum to be expected depend critically on the details of the ion-electron interaction and radiation processes assumed. This is unlike the case of the optically thick advection dominated flows, where gas and radiation are in approximate thermodynamic equilibrium. This is a source of uncertainty in the application of ISAFs to observed systems, since their radiative properties depend on poorly known quantities such as the strength of the magnetic field in the flow.

The various branches of optically thin and thick accretion flows are summarized in figure 4. Each defines a relation between surface density Σ (or optical depth $\tau = \kappa\Sigma$) and accretion rate. ISAFs require low densities, which can result either because of low accretion rates, or large values of the viscosity parameter. The condition that the cooling time of the ions by energy transfer to the electrons is longer than the accretion time yields a maximum accretion rate (Rees et al. 1982),

$$\dot{m} \lesssim \alpha^2, \quad (91)$$

where \dot{m} is the accretion rate in units of the Eddington value. If $\alpha \approx 0.05$ as suggested by current simulations of magnetic turbulence, the maximum accretion rate would be a few 10^{-3} .

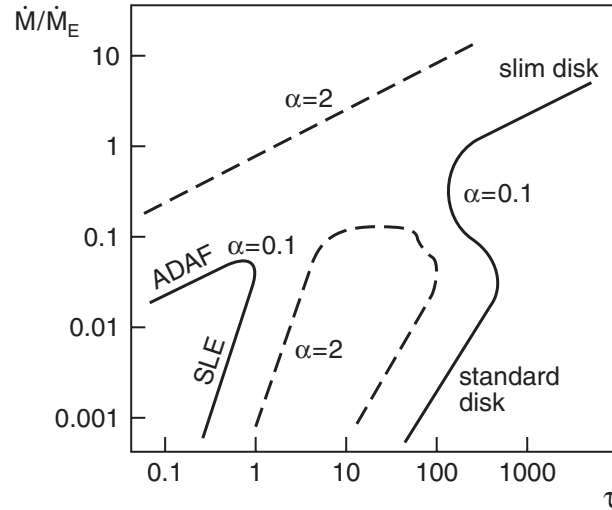


Fig. 4 Branches of advection-dominated and thin disks for two values of the viscosity parameter α , as functions of accretion rate and (vertical) optical depth of the flow (schematic, after Chen et al. 1995, Zdziarski 1998). Optically thin branches are the ISAF and SLE (Shapiro-Lightman-Eardley) solutions, optically thick ones the radiation dominated ('slim disk' or 'radiation torus') and SS (Shakura-Sunyaev or standard thin disk). Advection dominated are the ISAF and the radiation torus, geometrically thin are the SLE and SS. The SLE solution is a thermally unstable branch.

If ISAFs are to be applicable to systems with higher accretion rates, such as Cyg X-1 for example, the viscosity parameter must be larger, on the order of 0.3.

13.1 Application: hard spectra in X-ray binaries

In the hard state, the X-ray spectrum of black hole and neutron star accreters is characterized by a peak in the energy distribution (νF_ν or $E F(E)$) at photon energies around 100 keV. This is to be compared with the typical photon energy of ~ 1 keV expected from a standard optically thick thin disk accreting near the Eddington limit. The standard, and by far most likely explanation is that the observed hard photons are softer photons (around 1 keV) that have been up-scattered through inverse Compton scattering on hot electrons. Fits of such Comptonized spectra (e.g. Sunyaev and Titarchuk 1980, Zdziarski 1998 and references therein) yield an electron scattering optical depth around unity and an electron temperature of 50–100 keV. The scatter in these parameters is rather small between different sources. The reason may lie in part in the physics of Comptonization, but this is not the only reason. Something in the physics of the accretion flow keeps the Comptonization parameters fairly constant as long as it is in the hard state. ISAFs have been applied with some success in interpreting XRB. They can produce reasonable X-ray spectra, and have been used in interpretations of the spectral-state transitions in sources like Cyg X-1 (Esin et al. 1998 and references therein).

An alternative to the ISAF model for the hard state in sources like Cyg X-1 and the black hole X-ray transients is the ‘corona’ model. A hot corona (Bisnovatyi-Kogan and Blinnikov 1976), heated perhaps by magnetic fields as in the case of the Sun (Galeev et al. 1979) could be the medium that Comptonizes soft photons radiated from the cool disk underneath. The energy balance in such a model produces a Comptonized spectrum within the observed range (Haardt and Maraschi 1993). This model has received further momentum, especially as a model for AGN, with the discovery of broadened X-ray lines interpreted as indicative of the presence of a cool disk close to the last stable orbit around a black hole (Fabian et al. 2002 and references therein). The very rapid X-ray variability seen in some of these sources is interpreted as due magnetic flaring in the corona, like in the solar corona (e.g. Di Matteo et al. 1999a).

13.2 Transition from cool disk to ISAF: truncated disks

One of the difficulties in applying ISAFs to specific observed systems is the transition from a standard geometrically thin, optically thick disk, which must be the mode of mass transfer at large distances, to an ISAF at closer range. This is shown by figure 4, which illustrates the situation at some distance close to the central object. The standard disk and the optically thin branches are separated from each other for all values of the viscosity parameter. This separation of the optically thin solutions also holds at larger distances. Thus, there is no plausible continuous path from one to the other, and the transition between the two must be due to additional physics that is not included in diagrams like figure 4.

Circumstantial observational evidence points to the existence of such a transition. The distance from the hole where it is assumed to take place is then called the truncation radius. The extensive datasets from the black hole candidate Cyg X-1 obtained with the Rossi X-ray Timing Explorer (RXTE) have played an important role in the development of the truncated disk model. The X-ray spectrum of Cyg X-1 varies (on time scales of days to years) between softer and harder states, and the characteristic time scale of its fast variability (milliseconds to minutes) correlates closely with these changes. Since all disk time scales decrease with distance from the hole, the fast variability is interpreted as due to a process (still to be identified in detail) that depends on the size of the truncation radius. Variation in time of this radius is then assumed to cause the observed changes. Characteristics of the spectrum that find a natural place in this picture are: the slope of the hard X-ray spectrum, the amplitude of the so-called ‘Compton reflection hump’, and the behavior of the Fe K_{α} fluorescence line at 6.7 keV; each of these correlates with the characteristic fast variability time scale in an interpretable (though still somewhat model-dependent) way (Gilfanov et al. 1999, Revnivtsev et al. 1999). Very similar correlations have been found in X-ray observations of AGN (Zdziarski et al. 1999).

A promising possibility is that the transition takes place through *evaporation*. Two distinct mechanisms have been elaborated for such evaporation. In the first (Meyer and Meyer-Hofmeister 1994, Liu et al. 2002), the evaporation starts at a relatively large distance from the hole, where the virial temperature is of the order of $10^6 - 10^7$ K. As in the solar corona, the strong decrease of radiative efficiency of gas with temperature in this range produces a hot

optically thin corona in contact with the cool disk below, and exchange of mass can take place through evaporation and condensation, and the process is mediated by electron heat conduction. In this scenario, a corona flow at $\sim 10^7$ K at a distance of several hundred Schwarzschild radii transforms into a two-temperature ISAF further in.

13.2.1 Ion illumination

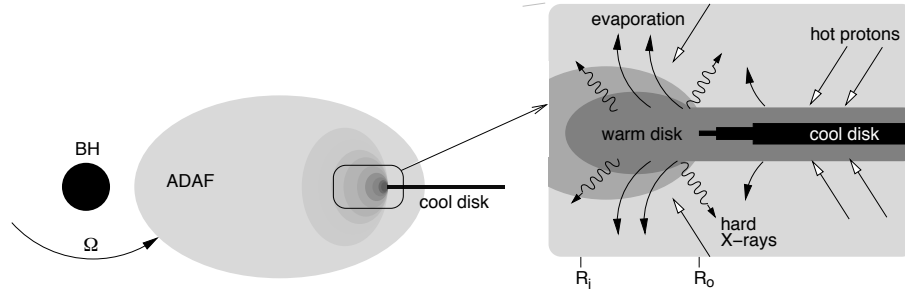


Fig. 5 interaction between ion supported accretion flow (ISAF) and cool disk in the truncated disk model for hard X-ray states in X-ray binaries. Accreting black hole on the left, its hot ions illuminating the cool disk create a warm (~ 100 keV surface layer producing the hard X-rays, extending inward and heating up to virial temperature by thermal instability ('evaporation') once cooling by soft photons becomes inefficient

Observations indicate that cool disks can also coexist with a hot, hard X-ray producing plasma quite close to the hole (for references see Dullemond and Spruit 2004). At these close distances, evaporation must behave differently from the coronal evaporation model, since the interaction of a two-temperature plasma with a cool disk is very different from that of a plasma at coronal temperatures (Spruit 1997). The energy in an ISAF is in the ions, and the electron conduction of heat that drives coronal evaporation unimportant. Moreover, the ions penetrate a substantial distance into the cool disk, and the energy they dump is radiated away long before they can heat up the disk to virial temperatures. Nevertheless, evaporation can still take place in this case, since it turns out that the interaction of the ions with the cool disk produces a layer of intermediate temperature (around 100 keV) that becomes thermally unstable in the presence of viscous dissipation, and heats up ISAF temperatures (Deufel et al. 2000, 2001, 2002, see also Spruit and Deufel 2002). The sequence of events is illustrated in figure 5. This model explains both the hard spectra of typical black hole accreters and the coexistence of cool and hot plasma that is indicated by the observations (Dullemond and Spruit 2004, D'Angelo et al. 2008).

13.3 Quiescent galactic nuclei

For very low accretion rates, such as inferred for the black hole in the center of our galaxy (identified with the radio source Sgr A*), the broad band spectral energy distribution of an ISAF is predicted to have two humps (Narayan et al. 1995, Quataert et al. 1999). In the X-ray range, the emission is due to bremsstrahlung. In the radio range, the flow emits synchrotron radiation, provided that the magnetic field in the flow has an energy density order of the gas pressure ('equipartition'). Synthetic ISAF spectra can be fitted to the observed radio and X-ray emission from Sgr A*. In other galaxies where a massive central black hole is inferred, and the center is populated by an X-ray emitting gas of known density, ISAFs would also be natural, and might explain why the observed luminosities are so low compared with the accretion rate expected for a hole embedded in a gas of the measured density.

13.4 ISAF-disk interaction: Lithium

One of the strong predictions of ISAF models, whether for black holes or neutron stars, is that the accreting plasma in the inner regions has an ion temperature of 10–100 MeV. Nearby is a cool and dense accretion disk feeding this plasma. If only a small fraction of the hot ion plasma gets in contact with the disk, the intense irradiation by ions will produce nuclear reactions (Aharonian and Sunyaev 1984, Martín et al. 1992). The main effects would be spallation of CNO elements into Li and Be, and the release of neutrons by various reactions. In this context, it is intriguing that the secondaries of both neutron star and black hole accreters have high overabundances of Li compared with other stars of their spectral types (Martín et al. 1992, 1994a). If a fraction of the disk material is carried to the secondary by a disk wind, the observed Li abundances may be accounted for (Martín et al. 1994b).

14 Outflows

The energy density in an advection dominated accretion flow is of the same order as the gravitational binding energy density GM/r , since a significant fraction of that energy went into internal energy of the gas by viscous dissipation, and little of it got lost by radiation. The gas is therefore only marginally bound in the gravitational potential. This suggests that perhaps a part of the accreting gas can escape, producing an outflow or wind. In the case of the ion supported ISAFs, this wind would be thermally driven by the temperature of the ions, like an 'evaporation' from the accretion torus. In the case of the radiation supported tori, which exist only at a luminosity near the Eddington value, but with much lower temperatures than the ion tori, winds driven by radiation pressure could exist.

The possibility of outflows is enhanced by the viscous energy transport through the disk. In the case of thin accretion disks (not quite appropriate in the present case, but sufficient to demonstrate the effect), the local rate of gravitational energy release ($\text{erg cm}^{-2}\text{s}^{-1}$) is $W = \Sigma v_r \partial_r (GM/r)$. The local viscous dissipation rate is $(9/4)v\Sigma\Omega^2$. As discussed in section

5.4 they are related by

$$Q_v = 3\left[1 - \left(\frac{r_i}{r}\right)^{1/2}\right]W, \quad (92)$$

where r_i is the inner edge of the disk. Part of the gravitational energy released in the inner disk is transported outward by the viscous stresses, so that the energy deposited in the gas is up to three times larger than expected from a local energy balance argument. The temperatures in an ADAF would be correspondingly larger. Begelman and Blandford (1999) have appealed to this effect to argue that in an ADAF most of the accreting mass of a disk might be expelled through a wind, the energy needed for this being supplied by the viscous energy transport associated with the small amount of mass that actually accretes.

Most outflows from disks such as the observed relativistic jets (and the non-relativistic ones in protostellar objects) are now believed to have a magnetic origin, requiring the presence of a strong, ordered (large scale) magnetic field anchored in the disk. Three-dimensional numerical MHD simulations of such processes are becoming increasingly realistic (e.g. Krolik & Hawley 2010, Moll 2009). The origin of jet-friendly magnetic field configurations, on the other hand, and the reasons for their apparently unpredictable presence are still unknown (not all black holes show jets, and the ones that do don't have them all the time). There is, however, a degree of correlation of their presence with the hard X-ray states in these objects (in the sense that they appear absent in soft states). For a discussion and interpretation of these issues see Spruit (2008).

References

- Abramowicz, M.A., Czerny B., Lasota J.-P., Szuszkiewicz E., 1988, *Astrophys. J.* **332**, 646
 Abramowicz M.A, Kato S., Matsumoto R., 1989, *Publ. Astr. Soc. Japan* **41**, 1215
 Aharonian F.A., Sunyaev, R.A., 1984 *Mon. Not. R. Astron. Soc.* **210**, 257
 Armitage P.J., 1998, *Astrophys. J.* **501**, L189
 Armitage P.J., and Livio M., 1998, *Astrophys. J.* **493**, 898
 Balbus S.A. and Hawley J.F., 1991, *Astrophys. J.* **376**, 214
 Balbus, S. A. 2003, *Ann. Rev. Astron. Astrophys.* **41**, 555
 Begelman M.C., 1979, *Mon. Not. R. Astron. Soc.* **187**, 237
 Begelman M.C., Meier D.L., 1982, *Astrophys. J.* **253**, 873
 Begelman M.C., McKee C.F., Shields G.A., 1983, *Astrophys. J.* **271**, 70
 Begelman M.C., Blandford R.D., 1999, *Mon. Not. R. Astron. Soc.* **303**, L1
 Bisnovatyi-Kogan G., 1993, *Astron. Astrophys.* **274**, 796
 Bisnovatyi-Kogan G., and Ruzmaikin A.A. 1976, *Ap. Space Sci.* **42**, 401
 Bisnovatyi-Kogan G.S., Blinnikov S.I., 1977, *Astron. Astrophys.* **59**, 111
 Bisnovatyi-Kogan G.S., Lamzin S.A., 1984, *Astron. Zh* **61**, 323 (translation *Soviet Astron.* **28**, 187)
 Blaes O. and Hawley J.F., 1988, *Astrophys. J.* **326**, 277
 Blandford R.D., 1976, *Mon. Not. R. Astron. Soc.* **176**, 465
 Blandford R.D. and Payne D.G., 1982 *Mon. Not. R. Astron. Soc.* **199**, 883
 Bondi H., 1952, *Mon. Not. R. Astron. Soc.* **112**, 195
 Bradshaw P., 1969, *J. Fluid Mech.* **36**, 177
 Brandenburg A., Nordlund Å., Stein R.F. and Torkelsson U., 1995, *Astrophys. J.* **446**, 741

- Cannon R.C., Eggleton P.P., Zytlow A.N., Podsiadlowski P., 1992, *Astrophys. J.* **386**, 206
- Cannizzo J.K., Shafter A.W., Wheeler J.C., 1988, *Astrophys. J.* **333**, 227
- Chen X.M., Abramowicz M.A., Lasota J.-P., Narayan R., Yi I., 1995, *Astrophys. J.* **443**, L61
- Chevalier R.A., 1993, *Astrophys. J.* **411**, 33
- D'Angelo, C., Giannios, D., Dullemond, C., & Spruit, H. 2008, *Astron. Astrophys.* **488**, 441
- D'Angelo, C. R., & Spruit, H. C. 2010, *Astron. Astrophys.* in press, arXiv:1001.1742
- Cordova F.A., 1995, in W.H.G. Lewin et al. eds. *X-ray Binaries*, Cambridge University Press, Cambridge, p.331
- Courant R. and Friedrichs K.O., 1948, *Supersonic Flow and Shock Waves*, Interscience, New York, and Springer, Berlin (1976)
- Chandrasekhar C., 1961, *Hydrodynamic and Hydromagnetic Stability*, Oxford Univ. Press, Oxford, and Dover Publications Inc., 1981
- Davis, S. W., Stone, J. M., & Pessah, M. E. 2010, *Astrophys. J.* **713**, 52
- De Villiers, J., & Hawley, J.F. 2003, *Astrophys. J.* **592**, 1060
- Di Matteo T., Celotti A., Fabian A.C., 1999a, *Mon. Not. R. Astron. Soc.* **304**, 809
- Di Matteo T., Fabian A. C., Rees M.J., Carilli C.L., Ivison R.J., 1999b, *Mon. Not. R. Astron. Soc.* **305**, 492
- Deufel, B., & Spruit, H. C. 2000, *Astron. Astrophys.* **362**, 1
- Deufel, B., Dullemond, C.P., & Spruit, H.C. 2001, *Astron. Astrophys.* **377**, 955
- Deufel, B., Dullemond, C.P., & Spruit, H.C. 2002, *Astron. Astrophys.* **387**, 907
- Dubrulle, B. 1992, *Astron. Astrophys.* **266**, 592
- Dullemond, C.P. & Spruit, H.C., 2005, *Astron. Astrophys.* **434**, 415
- Dullemond, C. P., Dominik, C., & Natta, A. 2001, *Astrophys. J.* **560**, 957
- Eardley D., and Lightman A., 1975, *Astrophys. J.* **200**, 187
- Emmering R.T., Blandford R.D., Shlosman I., 1992, *Astrophys. J.* **385**, 460
- Esin A.A., Narayan R., Cui W., Grove J.E., Zhang S.N., 1998, *Astrophys. J.* **505**, 854
- Fabian, A.C., et al. 2002, *Mon. Not. R. Astron. Soc.* **335**, L1
- Frank J., King A.R., and Raine D.J., 2002, *Accretion Power in Astrophysics* (3rd edition), Cambridge University Press.
- S. Fromang, J.C.B. Papaloizou, G. Lesur et al. 2007a, *Astron. Astrophys.* **476**, 1123
- Fromang, S., Papaloizou, J., Lesur, G., & Heinemann, T. 2007b, *Astron. Astrophys.* **476**, 1123
- Galeev A.A., Rosner R., Vaiana G.S., 1979, *Astrophys. J.* **229**, 318
- Gammie, C. F. 1997, IAU Colloq. 163: Accretion Phenomena and Related Outflows, ed. D. T. Wickramasinghe et al. 121, 704
- Gilfanov, M., Churazov, E., & Revnivtsev, M. 1999, *Astron. Astrophys.* **352**, 182
- Gilham S., 1981, *Mon. Not. R. Astron. Soc.* **195**, 755
- Haardt F., Maraschi L., Ghisellini G., 1994, *Astrophys. J.* **432**, 95
- Hameury J.-M., Menou K., Dubus G., Lasota J.-P., Hure J.-M., 1998, *Mon. Not. R. Astron. Soc.* **298**, 1048
- Hawley J.E., 1991 *Astrophys. J.* **381**, 496
- Hawley J.F., Gammie C.F. and Balbus S.A., 1995, *Astrophys. J.* **440**, 742
- Hawley J.F., Balbus S.A., Winters W.F. 1999, *Astrophys. J.* **518**, 394
- Hawley, J. F., Balbus, S. A., & Winters, W. F. 1999, *Astrophys. J.* **518**, 394
- Hirose, S., Krolik, J.H., De Villiers, J., & Hawley, J.F. 2004, *Astrophys. J.* **606**, 1083
- Hirose, S., Krolik, J. H., & Blaes, O. 2009, *Astrophys. J.* **691**, 16

- Honma F., Kato S., Matsumoto R., Abramowicz M., 1991, *Publ. Astr. Soc. Japan* **43**, 261
- Horne K., 1985, *Mon. Not. R. Astron. Soc.* **213**, 129
- Horne, K., 1993, in J.C. Wheeler, ed., *Accretion Disks in Compact Stellar Systems*, Singapore: World Scientific Publishing
- Hōshi R., 1979, *Prog. Theor. Phys.* **61**, 1307
- Hurley, K., et al. 2005, *Nature* **434**, 1098
- Ichimaru S., 1977, *Astrophys. J.* **241**, 840
- Igumenshchev I.V., Chen X.M., Abramowicz A., 1996 *Mon. Not. R. Astron. Soc.* **278**, 236
- Igumenshchev I.V., Abramowicz M.A., 1999, *Mon. Not. R. Astron. Soc.* **303**, 309
- Illarionov A.F., Sunyaev R.A., 1975, *Astron. Astrophys.* **39**, 185
- Inogamov N.A., Sunyaev R.A., 1999, *Astron. Lett.*, 1999, 25, 269 (=astro-ph/9904333)
- Ji, H., Burin, Scharfman, M.E. & J. Goodman, J., 2006, *Nature* **444**, 343
- Kato M., 1997, *Astrophys. J. Suppl.* **113**, 121
- Kippenhahn R. and Thomas H.-C., 1981, in D. Sugimoto, D. Lamb and D.N. Schramm, *Fundamental Problems in the Theory of Stellar Evolution* (IAU Symp. **93**), Reidel, Dordrecht, p.237
- King A.R., 1995 in Lewin, W.H.G., van Paradijs, J., van den Heuvel, E.P.J., eds., *X-ray Binaries*, Cambridge University press
- King, A. R. 2004, *Mon. Not. R. Astron. Soc.* **347**, L18
- King A.R. and Ritter H., 1999 *Mon. Not. R. Astron. Soc.* **309**, 253
- King A.R., Begelman M.C., 1999, *Astrophys. J.* **519**, L169
- Königl A., 1989 *Astrophys. J.* **342**, 208
- Königl A., Kartje J.F., 1994 *Astrophys. J.* **434**, 446
- Klahr, H. H., & Bodenheimer, P. 2003, *Astrophys. J.* **582**, 869
- Kley W., 1991, *Astron. Astrophys.* **247**, 95
- Kley,W., Papaloizou J.C.B., Lin D.N.C, 1993, *Astrophys. J.* **416**, 679
- Krolik, J. H., & Hawley, J. F. 2010, *Lecture Notes in Physics*, Berlin: Springer **794**, 265
- Kuulkers E., Howell S.B., van Paradijs J., 1996, *Astrophys. J.* **462**, 87
- Landau L.D. and Lifshitz E.M., 1959 *Fluid Mechanics*, Pergamon Press, Oxford
- Lee, C.-F., Mundy, L. G., Reipurth, B., Ostriker, E. C., & Stone, J. M. 2000, *Astrophys. J.* , **542**, 925
- Lesur, G., & Longaretti, P.-Y. 2005, *Astron. Astrophys.* **444**, 25
- Lesur, G., & Ogilvie, G. I. 2008, *Astron. Astrophys.* **488**, 451
- Lesur, G., & Papaloizou, J. C. B. 2010, *Astron. Astrophys.* **513**, A60
- Lewin W.H.G., van Paradijs J., van den Heuvel E.P.J., 1995, *X-ray Binaries*, Cambridge University press
- Lightman A.P., Eardley D.M., 1974, *Astrophys. J.* **187**, L1
- Lin D.N.C., and Taam R.E., 1984, in S.E. Woosley, ed., *High Energy Transients in Astrophysics*, AIP Conference Procs. **115**, p.83
- Liu, B.F., Mineshige, S., Meyer, F., Meyer-Hofmeister, E., & Kawaguchi, T. 2002, *Astrophys. J.* **575**, 117
- Long, M., Romanova, M. M., & Lovelace, R. V. E. 2008, *Mon. Not. R. Astron. Soc.* **386**, 1274
- Lovelace R.V.E., 1976, *Nature* **262**, 649
- Lüst R., 1952, *Z. Naturforsch.* **7a**, 87
- Lynden-Bell D. and Pringle J.E., 1974, *Mon. Not. R. Astron. Soc.* **168**, 603

- Lyutiy V.M. and Sunyaev R.A., 1976, *Astron. Zh.* **53**, 511, translation in *Sov. astron.* **20**, 290 (1976)
- Martín E L., Rebolo R., Casares J., Charles P.A., 1992, *Nature* **358**, 129
- Martín E.L., Rebolo R., Casares J., Charles P.A., 1994a *Astrophys. J.* **435**, 791
- Martín E., Spruit H.C., van Paradijs J., 1994b, *Astron. Astrophys.* **291**, L43
- Massey B.S., 1968, *Mechanics of Fluids*, Chapman and Hall, London (6th Ed. 1989)
- Meyer F., 1990, *Rev. Mod. Astron.* **3**, 1
- Meyer F. and Meyer-Hofmeister E., 1981, *Astron. Astrophys.* **104**, L10
- Meyer F. and Meyer-Hofmeister E., 1982, *Astron. Astrophys.* **106**, 34
- Meyer-Hofmeister, E. and Ritter, H., 1993, in *The Realm of Interacting Binary Stars*, ed. J. Sahade, Kluwer, Dordrecht, p.143
- Meyer F., Meyer-Hofmeister E., 1994, *Astron. Astrophys.* **288**, 175
- Meyer-Hofmeister E., Schandl S., and Meyer F., 1997 *Astron. Astrophys.* **318**, 73
- Meyer-Hofmeister E., Meyer F., 1999, astro-ph/9906305
- Migliari, S., & Fender, R. P. 2006, *Mon. Not. R. Astron. Soc.* **366**, 79
- Miller, K.A., and Stone, J.M., 1997, *Astrophys. J.* **489**, 890
- Mineshige S. and Wheeler J.C., 1989 *Astrophys. J.* **343**, 241
- Mineshige S., and Wood J.A., 1989, in *Theory of Accretion Disks*, eds. F. Meyer, W. Duschl, J. Frank and E. Meyer-Hofmeister, Kluwer, Dordrecht, p.221
- Moll, R. 2009, *Astron. Astrophys.* **507**, 1203
- Nakamura K.E., Matsumoto R., Kusunose M., Kato S., 1996, *Publ. Astr. Soc. Japan* **48**, 769
- Narayan R., Goldreich P., Goodman, J., 1987, *Mon. Not. R. Astron. Soc.* **228**, 1
- Narayan R. and Popham R., 1993, in *Theory of Accretion Disks II*, eds. W. Duschl et al., Kluwer Dordrecht, p293
- Narayan R., Yi I., 1994, *Astrophys. J.* **428**, L13
- Narayan R., Yi I., Mahadevan R., 1995, *Nature* **374**, 623
- Narayan R., Kato S., Honma F., 1997, *Astrophys. J.* **476**, 49
- O'Donoghue D.O., Chen A., Marang F., Mittaz P.D., Winkler H., Warner B. 1991, *Mon. Not. R. Astron. Soc.* **250**, 363
- Ogilvie G.I., 1999, *Mon. Not. R. Astron. Soc.* **306**, L9
- Osaki Y., 1974, *Publ. Astr. Soc. Japan* **26**, 429
- Ostriker E.C., Gammie C.F., Stone J.M., 1999, *Astrophys. J.* **513**, 259
- Osaki Y., 1993 in *Theory of Accretion Disks, II*, eds. W. Duschl et al., Kluwer Dordrecht, p93
- Paczynski B., 1978, *Acta Astron.* **28**, 91
- Paczynski B., 1991, *Astrophys. J.* **370**, 597
- Paczynski, B. 1998, *Astrophys. J. Letters* **494**, L45
- Papaloizou, J. C. B., & Lin, D. N. C. 1995, *Ann. Rev. Astron. Astrophys.* , 33, 505
- Piran T., 1978, *Astrophys. J.* **221**, 652
- Podolak M., Hubbard W.B. Pollack J.B., 1993, in *Protostars and Planets II*, University of Arizona Press, p.1109
- Popham R. and Narayan R., 1991, *Astrophys. J.* **370**, 604
- Popham R., Woosley S.E., Fryer C., 1999, *Astrophys. J.* **518**, 356
- Popham R., 1997, in *Accretion Phenomena and related Outflows (IAU Colloquium 163)*, ASP Conference Series 121, ed. D. T. Wickramasinghe; G.V. Bicknell; and L. Ferrario, p.230

- Pringle J.E., 1981 *Ann. Rev. Astron. Astrophys.* **19**, 137
- Pringle J.E. and Savonije, G.J., 1979, *Mon. Not. R. Astron. Soc.* **187**, 777
- Quataert E., Narayan R., 1999 *Astrophys. J.* **517**, 101
- Rafikov, R. R. 2009, *Astrophys. J.* , 704, 281
- Rappaport S., Podsiadlowski P., 2000, *Astrophys. J.* **529**, 946
- Rappaport, S.A., Fregeau, J.M., Spruit, H.C., 2004, *Astrophys. J.* **606**, 436
- Różyczka M. and Spruit H.C., 1993, *Astrophys. J.* **417**, 677 (with video)
- Rees M.J., 1978, *Physica Scripta* **17**, 193
- Rees M.J., Phinney E.S., Begelman M.C., Blandford R.D., 1982, *Nature* **295**, 17
- Regev, O., Hougerat, A. 1988, *Mon. Not. R. Astron. Soc.* **232**, 81
- Revnitvsev, M., Gilfanov, M., & Churazov, E. 1999, *Astron. Astrophys.* **347**, L23
- Rincon, F., Ogilvie, G. I., & Cossu, C. 2007, *Astron. Astrophys.* **463**, 817
- Rybicki G.R. and Lightman A.P., 1979, *Radiative Processes in Astrophysics*, Wiley, New York, Ch 1.5
- Rutten R., van Paradijs J., Tinbergen J., 1992, *Astron. Astrophys.* **260**, 213
- Sakimoto P., Coroniti F.V., 1989, *Astrophys. J.* **342**, 49
- Sawada K., Matsuda T., Inoue M. & Hachisu 1987, *Mon. Not. R. Astron. Soc.* **224**, 307
- Schandl S., Meyer F., 1994, *Astron. Astrophys.* **289**, 149
- Schandl S., Meyer F., 1997, *Astron. Astrophys.* **321**, 245
- Schultz A.L., Price R.H., 1985, *Astrophys. J.* **291**, 1
- Shakura N.I. and Sunyaev R.A., 1973, *Astron. Astrophys.* **24**, 337
- Shi, J., Krolik, J. H., & Hirose, S. 2010, *Astrophys. J.* **708**, 1716
- Sunyaev R.A., Shakura N.I., 1977, *Pi'sma Astron. Zh.* **3**, 262 (translation *Soviet Astron. L.* **3**, 138)
- Shapiro S.L., Lightman A.P., Eardley D.M., 1976 *Astrophys. J.* **204**, 187
- Smak J., 1971, *Acta Astron.* **21**, 15
- Smak J., 1984, *Publ. Astr. Soc. Pac.* **96**, 54
- Spitzer L., 1965, *Physics of fully ionized gases*, Interscience Tracts on Physics and Astronomy, New York: Interscience Publication, 1965, 2nd rev.
- Spruit H.C., 1987, *Astron. Astrophys.* **184**, 173
- Spruit H.C. 1996, in *Evolutionary Processes in Binary Stars*, R.A.M.J. Wijers et al. (eds.), NATO ASI C **477**, Kluwer Dordrecht, p249
- Spruit H.C., Rutten R.G.M., 1998, *Mon. Not. R. Astron. Soc.* **299**, 768
- Spruit H.C., Matsuda T., Inoue M., Sawada K., 1987, *Mon. Not. R. Astron. Soc.* **229**, 517
- Spruit H.C., Taam R.E., 1993, *Astrophys. J.* **402**, 593
- Spruit H.C., 1997, in *Accretion disks-new aspects*, eds. E. Meyer-Hofmeister and H.C. Spruit, *Lecture Notes in Physics* **487**, Springer, p. 67
- Spruit, H.C., & Deufel, B. 2002, *Astron. Astrophys.* **387**, 918
- Spruit, H.C., 2008, arXiv:0804.3096v4 [astro-ph]
- Spruit, H.C., 2010, arXiv:1004.4545
- Strom S.E., Edwards S., Skrutskie M.F., 1993, in *Protostars and Planets III*, eds. E.H. Levy, J.I. Lunine, Univ. Arizona Press, Tucson, p.837
- Sunyaev R.A., Shakura N.I., 1977, *PAZh* **3**, 262 it *Soviet Astron. Letters* **3**, 138
- Sunyaev, R. A., & Titarchuk, L. G. 1980, *Astron. Astrophys.* **86**, 121

- Taam R.E., 1994, in Compact stars in Binaries (IAU Symp **165**), J. van Paradijs et al. eds., Kluwer, p.3
- Taam, R. E., & Sandquist, E. L. 2000, *Ann. Rev. Astron. Astrophys.* **38**, 113
- Treves A., Maraschi L., and Abramowicz M., 1988 *Publ. Astr. Soc. Pac.* **100**, 427
- Turner, N. J. 2004, *Astrophys. J. Letters* **605**, L45
- Turner, N. J., Blaes, O. M., Socrates, A., Begelman, M. C., & Davis, S. W. 2005, *Astrophys. J.* **624**, 267
- van Paradijs J. and McClintock J.E., 1995, in Lewin, W.H.G., van Paradijs, J. and van den Heuvel, E.P.J., eds., *X-ray Binaries*, Cambridge Univ. Press, Cambridge, p.58
- van Paradijs J, Verbunt F. 1984, in S.E. Woosley, ed., *High Energy Transients in Astrophysics*, AIP Conference Procs. **115**, p.49
- Velikhov, 1959, *J. Expl. Theoret. Phys.* (USSR), **36**, 1398
- Wang J.M., Zhou Y.Y., 1999 *Astrophys. J.* **516**, 420
- Warner B. 1987, *Mon. Not. R. Astron. Soc.* **227**, 23
- Warner B. 1995, *Cataclysmic Variable Stars*, Cambridge: CUP
- Wood J.A., Horne K., Berriman G, Wade R.A. 1989a *Astrophys. J.* **341**, 974
- Wood J.A., Marsh T.R., Robinson E.L. et al., 1989b, *Mon. Not. R. Astron. Soc.* **239**, 809
- Wood J.H., Horne K., Vennes S., 1992, *Astrophys. J.* **385**, 294
- Woosley, S. E. 1993, *Astrophys. J.* **405**, 273
- Yi I., 1999, in *Astrophysical Discs*, eds. J.A. Sellwood and J. Goodman, Astronomical Society of the Pacific Conference series *160*, 279. (astro-ph/9905215)
- Zdziarski A.A., 1998, *Mon. Not. R. Astron. Soc.* **296**, L51
- Zdziarski, A. A., Lubinski, P., & Smith, D. A. 1999, *Mon. Not. R. Astron. Soc.* **303**, L11
- Zel'dovich Ya. B., 1981, *Proc. Roy. Soc. London* **A374**, 299